Cell

# Mutant p53 Drives Pancreatic Cancer Metastasis through Cell-Autonomous PDGF Receptor β Signaling

Susann Weissmueller,[1,2,11] Eusebio Manchado,[2,11] Michael Saborowski,[2] John P. Morris IV,[2] Elvin Wagenblast,[1] Carrie A. Davis,[1] Sung-Hwan Moon,[3] Neil T. Pfister,[3] Darjus F. Tschaharganeh,[2] Thomas Kitzing,[2] Daniela Aust,[4] Elke K. Markert,[5] Jianmin Wu,[6,7] Sean M. Grimmond,[8,9] Christian Pilarsky,[4] Carol Prives,[3] Andrew V. Biankin,[6,9] and Scott W. Lowe[1,2,10,*]

[1]Watson School of Biological Sciences, Cold Spring Harbor Laboratory, Cold Spring Harbor, NY 11724, USA
[2]Department of Cancer Biology and Genetics, Memorial Sloan-Kettering Cancer Center, New York, NY 10065, USA
[3]Department of Biological Sciences, Columbia University, New York, NY 10027, USA
[4]Department of Visceral, Thoracic and Vascular Surgery, Technical University of Dresden, 01062 Dresden, Germany
[5]The Simons Center for Systems Biology, Institute for Advanced Study, Princeton, NJ 08540, USA
[6]The Kinghorn Cancer Centre, Cancer Division, Garvan Institute of Medical Research, Sydney NSW 2010, Australia
[7]St Vincent's Clinical School, University of New South Wales, Sydney, NSW 2010, Australia
[8]Queensland Centre for Medical Genomics, Institute for Molecular Bioscience, University of Queensland, Santa Lucia 4072, Australia
[9]Wolfson Wohl Cancer Research Centre, Institute of Cancer Sciences, University of Glasgow, Scotland G61 1BD, UK
[10]Howard Hughes Medical Institute, New York, NY 10065, USA
[11]Co-first author
*Correspondence: lowes@mskcc.org
http://dx.doi.org/10.1016/j.cell.2014.01.066

## SUMMARY

Missense mutations in the *p53* tumor suppressor inactivate its antiproliferative properties but can also promote metastasis through a gain-of-function activity. We show that sustained expression of mutant p53 is required to maintain the prometastatic phenotype of a murine model of pancreatic cancer, a highly metastatic disease that frequently displays *p53* mutations. Transcriptional profiling and functional screening identified the platelet-derived growth factor receptor b (PDGFRb) as both necessary and sufficient to mediate these effects. Mutant p53 induced PDGFRb through a cell-autonomous mechanism involving inhibition of a p73/NF-Y complex that represses PDGFRb expression in p53-deficient, noninvasive cells. Blocking PDGFRb signaling by RNA interference or by small molecule inhibitors prevented pancreatic cancer cell invasion in vitro and metastasis formation in vivo. Finally, high PDGFRb expression correlates with poor disease-free survival in pancreatic, colon, and ovarian cancer patients, implicating PDGFRb as a prognostic marker and possible target for attenuating metastasis in p53 mutant tumors.

## INTRODUCTION

Mutations in the *p53* tumor suppressor gene represent the most common genetic lesions in cancer (Freed-Pastor and Prives, 2012). Functional studies indicate that wild-type p53 possesses a series of antiproliferative activities that limit the proliferation and survival of premalignant cells. p53 exerts these activities, at least in part, through its ability to bind DNA in a sequence-specific manner to regulate gene expression, and the vast majority of mutations that occur in human tumors disable this property of p53 and, consequently, its antiproliferative effects.

*p53* mutations typically occur within the DNA-binding region and involve either DNA contact residues or residues important for conformational structure, both resulting in loss of DNA binding (Joerger and Fersht, 2007). Because p53 functions as a tetrameric transcription factor, mono-allelic *p53* mutations can exert dominant-negative effects on a coexpressed wild-type p53 protein. p53 activates E3 ubiquitin ligases that feed back to trigger p53 destruction and its rapid turnover; however, p53 missense mutants defective in regulating gene expression lead to the stable accumulation of the variant proteins (Oren and Rotter, 2010). Interestingly, genetically engineered mice harboring common *p53* point mutations develop more aggressive and metastatic tumors compared to those arising in their *p53* heterozygous or null counterparts (Lang et al., 2004; Olive et al., 2004, Hanel et al., 2013), suggesting that the mutant forms of p53 exert gain-of-function activities independent of their effects on wild-type p53. Accordingly, human tumors with mutant *p53* are associated with poor patient prognosis (Soussi and Béroud, 2001) and drug resistance (Masciarelli et al., 2013).

Recently, targeting mutant p53 function has been proposed as an antimetastatic measure. As p53 mutant proteins have to date proved undruggable (Levine and Oren, 2009; Lehmann and Pietenpol, 2012), efforts have focused on identifying the underlying mechanisms that mediate its effects. Such efforts have identified proteins involved in integrin recycling (Muller et al., 2009), the mevalonate pathway (Freed-Pastor et al., 2012), or microRNA

(miRNA) biogenesis (Su et al., 2010) as potential mediators of mutant p53 action in invasion and metastasis. So far, most studies have been performed in breast cancer, and the proposed mechanisms do not necessarily validate across cancer types. These observations underscore the importance of the cellular context in assessing mutant p53 action and highlight the potential complexity of the effector network.

Pancreatic ductal adenocarcinoma (PDAC) is one cancer type in which mutant *p53* impacts disease progression. PDAC arises from indolent pancreatic intraepithelial neoplasias (PanINs) that frequently go undetected and persist for many years. However, the conversion of PanINs to highly aggressive, frankly invasive and metastatic PDACs, in which *p53* is mutated in 75% of cases, carries a dire prognosis because of late-stage detection, the presence of metastases, and ineffective treatment options (Li et al., 2004). Even those patients with a surgically approachable pancreatic lesion develop recurrent and metastatic disease after local tumor resection (Hidalgo, 2010). Consistent with a role for mutant p53 in this process, mice harboring pancreatic cancers driven by oncogenic *Kras* and a mutant *p53* allele show more metastases compared to identical mice harboring a *p53* null allele (Morton et al., 2010). However, it is not known whether mutant p53 is needed to sustain the metastatic phenotype and how it is regulated. Such information would produce insights into p53 action and validate mutant p53 as a therapeutic target.

In this study, we combined several orthogonal approaches and models to systematically explore the molecular basis whereby mutant p53 promotes invasion and metastasis in PDAC and the clinical implications of its effects. These studies identified the platelet-derived growth factor receptor β (PDGFRb) as necessary and sufficient to mediate the effects of mutant p53 on invasion and metastasis in both a murine model and human PDAC cells. Further, we identified elevated PDGFRb expression as an indicator of poor metastasis-free survival in human PDAC patients. Taken together, our data identify a key mediator of mutant p53 activity and suggest that PDGFRb inhibitors may act as antimetastatic agents in some patients with tumors expressing mutant p53.

## RESULTS

### Sustained Expression of Mutant p53 Is Required for the Invasive Phenotype of Pancreatic Cancer Cells

Genetically engineered mouse models of pancreatic cancer harboring a latent oncogenic *Kras* allele (*lox-stop-lox* $Kras^{G12D}$), a latent mutant $p53^{R172H}$, and a tissue-specific *Cre* recombinase (*Pdx1-Cre*), also known as KPC mice, develop highly metastatic pancreatic cancer that faithfully mimics the human disease (Hingorani et al., 2005). To understand the impact of *p53* mutations on cell invasion and metastasis in this well-defined genetic system, we employed a murine KPC pancreatic cancer cell line that lost the remaining *p53* wild-type allele during disease progression (Morton et al., 2010). The behavior of KPC cell lines stably expressing small hairpin RNAs (shRNAs) targeting (mutant) *p53*, or control shRNAs targeting *Renilla* (KPC+sh.Ctrl), were compared to one another and to a *p53* null $KP_{fl}C$ cell line (from a *Pdx-Cre*, *LSL-*$Kras^{G12D/+}$, *LSL-*$p53^{loxP/+}$) expressing the control shRNA ($KP_{fl}C$+sh.Ctrl).

We confirmed that KPC+sh.Ctrl cells expressing mutant p53 efficiently migrated in scratch-wound assays. This motility depended on mutant p53, as mutant p53 knockdown in KPC+sh.p53 cells reduced motility similarly to $p53^{-/-}$ $KP_{fl}$C+sh.Ctrl cells (Figure 1A). Next, we examined the invasive capacity of KPC cells into collagen gels in an inverted invasion assay. The presence of mutant p53 in KPC+sh.Ctrl cells enhanced invasiveness, which was significantly abrogated upon p53 knockdown (Figure 1B). The ability of mutant p53 to drive cell invasion was also evident following enforced expression of $p53^{R175H}$ and $p53^{R273H}$, two mutants frequently found in human PDAC, in $KP_{fl}C$ cells. This result indicates that the differences in invasiveness of KPC and $KP_{fl}C$ cells depend on mutant p53 and were not acquired during generation and selection of cell populations expressing shRNAs or through RNAi off-target effects.

To test whether mutant p53 expression was required to sustain the metastatic potential of KPC cells, we orthotopically injected KPC+sh.Ctrl and KPC+sh.p53 cells into the pancreata of athymic mice and scored the number of metastases formed in both lung and liver, the most common sites of pancreatic cancer spread in patients. Although the primary tumor burden was independent of p53 status, tumors originating from KPC+sh.Ctrl cells expressing mutant p53 were significantly more metastatic than those in which mutant p53 was silenced, and metastases in the lung and liver were detected to a greater extent in mice that had been injected with cells expressing mutant p53 (Figure 1C). Together, these results demonstrate that mutant p53 can contribute to PDAC invasion and metastasis and that inhibiting its activity can have an antimetastatic effect.

### Transcriptional Profiling and Functional Screening Identify PDGFRb as a Downstream Mediator of Mutant p53 in Murine Pancreatic Cancer

To gain insight into how mutant p53 mediates the invasive phenotype of PDAC, we performed genome-wide transcriptome profiling of KPC cells by RNA sequencing (RNA-seq). Four days following knockdown of mutant p53 in three independent clonal KPC populations, we observed a complex pattern of gene expression changes compared to three independent KPC+sh.Ctrl cell lines. We identified 441 genes either significantly up- or downregulated upon shRNA-mediated depletion of endogenous mutant p53 (Figure 2A; Figure S1A available online). Ingenuity pathway analysis revealed that ~20% of the affected genes fall into the functional class of "cellular movement," supporting our experimental observations that mutant p53 can govern the invasive phenotype of pancreatic cancer cells (Figures 2B and S1C).

To facilitate the identification of mediators of mutant p53 activity, we focused on genes whose expression was positively regulated by mutant p53, as such molecules might both mediate effects of mutant p53 and be targets for pharmacological inhibition. Therefore, we generated pools of 3–6 shRNAs targeting individual upregulated genes, and we screened them one-by-one to identify those that phenocopied the decreased invasion seen upon downregulation of mutant p53 (Table S1). We identified three genes whose knockdown abrogated invasion driven by mutant p53 (Figure 2C). SLC40A1 is a cell membrane protein

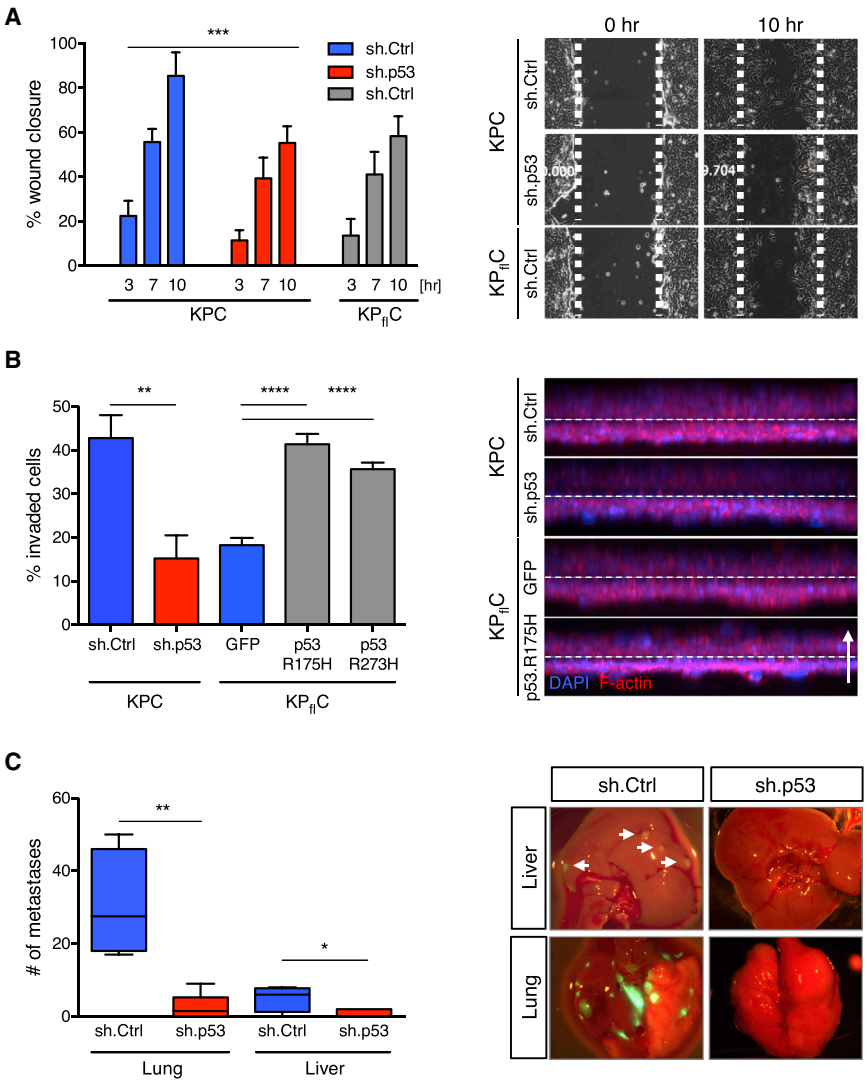


**Figure 1. Depletion of Mutant p53 Abrogates Invasiveness of Pancreatic Cancer Cells**

(A) Quantification of wound distances in scratch-wound assays from 0, 3, 7, and 10 hr after wounding of KPC cells stably expressing a non-targeting control shRNA (sh.Ctrl) or a shRNA-targeting mutant p53 (sh.p53) or $KP_{fl}C$ cells stably expressing a sh.Ctrl (left panel). Data presented as mean ± SD. ***$p < 0.001$. Representative phase contrast images from live cell recordings of each condition are shown at 0 and 10 hr (right panel).

(B) KPC+sh.p53, +sh.Ctrl, and $KP_{fl}C$ cells expressing the GFP control and mutant p53 (175H and 273H) vector were allowed to invade into collagen for 72 hr before quantification as described in the Experimental Procedures (left panel). The average of invaded cells from nine replicates ± SD is shown. A representative result of three repeated experiments is shown. **$p < 0.01$, ****$p < 0.0001$. Representative three-dimensional (3D) reconstructions of each condition are shown (right panel). Cells were stained for F-actin (red) and DAPI (blue); the dashed line indicates the approximate position of the Transwell membrane; and the arrow indicates the direction of movement.

(C) KPC+sh.p53 or +sh.Ctrl cells were orthotopically injected into the pancreata of athymic mice. When symptomatic, mice were euthanized, and metastatic spread in lung and liver was quantified by counting GFP-positive macroscopic nodules (left panel). Data presented as mean ± SD. *$p < 0.05$, **$p < 0.01$. Panels show representative merged brightfield/GFP images from lung and liver (right panel).

that has been shown to mediate cellular iron efflux (Montalbetti et al., 2013); SNED1 is a stromal marker that induces cisplatin-resistance in head and neck squamous carcinoma (Longati et al., 2013); and PDGFRb is a receptor tyrosine kinase that mediates PDGF-regulated proliferation, survival, and chemotaxis (Dai, 2010).

Oncogenic properties of mutated or amplified PDGFRa have been extensively studied in several tumor types, whereas PDGFRb has been exclusively linked to tumor angiogenesis via paracrine effects (Pietras et al., 2003; Cao et al., 2004). Based on our screening results, we hypothesized that PDGFRb may also have a cell-autonomous impact on cell invasion in pancreatic cancer. First, we verified by qRT-PCR and western blotting that PDGFRb mRNA and protein were reduced upon knockdown of mutant p53 (Figures 2D and 2E). Expression of mutant p53 correlated with high PDGFRb expression levels and also with the expression of key downstream mediators of the PDGFRb signaling cascade (Figure S1B).

We next examined the effects of depleting each PDGFR isoform on the invasive potential of KPC cells in vitro (Figure 3A). Although knockdown of PDGFRa had no effect, depletion of PDGFRb decreased the ability of KPC cells to invade (Figure 3B). Conversely, overexpression of PDGFRb in $p53^{-/-}$ $KP_{fl}C$ enhanced cell migration and invasion, similarly to cells overexpressing mutant forms of p53 (Figure S2A). Reduced levels of PDGFRb in KPC cells neither altered the rate of cell proliferation (Figure S2B) nor led to a competitive proliferative disadvantage over KPC cells expressing high PDGFRb levels (Figure S2C). When GFP-positive KPC+sh.PDGFRb cells were mixed with dsRED-positive KPC+sh.Ctrl cells and injected subcutaneously into athymic mice, the GFP:dsRED ratio of pre-injected cells was maintained in the established tumors, indicating that increased PDGFRb levels did not confer a selective advantage to tumor cell proliferation at the site of injection (Figure S2D). Thus, cell-autonomous activity of PDGFRb is not required for the proliferation and tumorigenic potential of p53 mutant murine cancer cells but specifically impacts their invasive potential.

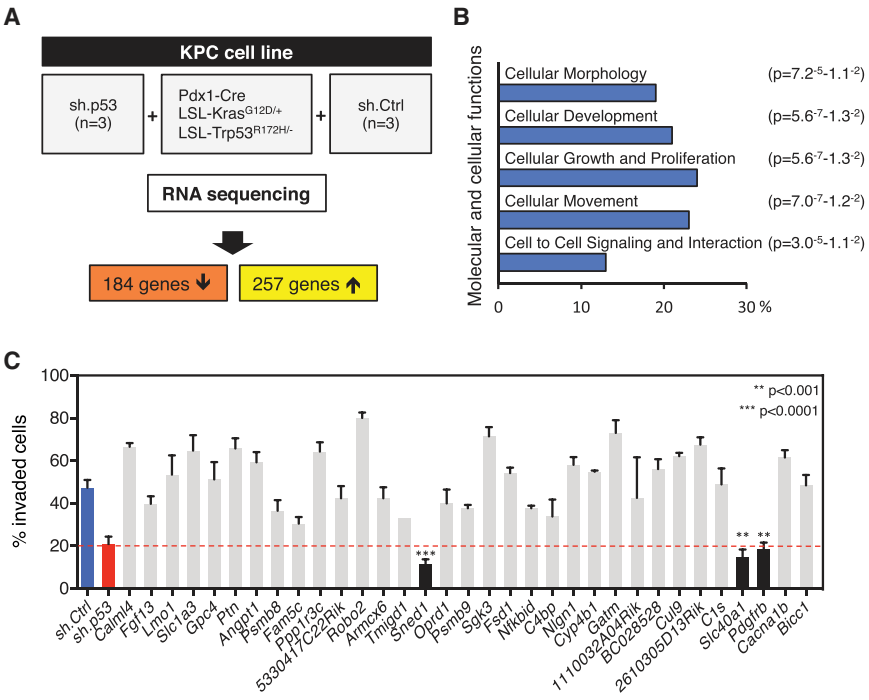


**Figure 2. Identification of PDGFRb as a Downstream Mediator of Mutant p53 in Regulating Cell Invasion**

(A) Schematic workflow of RNA sequencing.

(B) Ingenuity pathway analysis (Ingenuity Systems, http://www.ingenuity.com). Bars ($p < 0.05$) represent molecular and cellular functions that are significantly changed following mutant p53 depletion.

(C) One-by-one invasion assay screen. Quantification of invaded KPC cells infected with individual shRNA-pools (~3.6 shRNAs/gene) targeting the top 40 upregulated genes identified by RNA-seq. Data presented as mean ± SD.

(D) qRT-PCR for PDGFRb in KPC+sh.p53 (2 or 3) or +sh.Ctrl cells. Data presented as mean normalized PDGFRb expression ± SD of triplicate samples. $^{**}p < 0.01$, $^{***}p < 0.001$. A representative result of three repeated experiments is shown.

(E) Western blotting analysis of PDGFRb, p53, and actin in sh.p53- or sh.Ctrl-expressing KPC cells. The two bands of PDGFRb represent differentially glycosylated forms of the protein.

See also Figure S1 and Table S1.

## PDGFRb Mediates Mutant p53 Action in Human Cancer Cells

To determine if the mutant p53-PDGFRb signaling axis acts in human cancer cells, we analyzed PDGFRb expression levels in a panel of human pancreatic cancer cell lines. As in our model, PDGFRb mRNA levels were significantly higher in cells expressing mutant p53 compared to those in cell lines that maintained or lost the wild-type *p53* allele (Figure 3C). Furthermore, knockdown of mutant *p53* in Miapaca2, BXPC3, CFPAC, and A2.1 cell lines (carrying the 248W, 220C, 242R, and 155P alleles, respectively) decreased PDGFRb mRNA levels to varying degrees (Figure 3D). Knockdown of mutant p53 also decreased PDGFRb expression in several human colon (SW620, p53$^{273H/P309S}$), lung (H1975, p53$^{273H}$), and breast (MDA-MB-231, p53$^{280K}$) cancer cell lines (Figure S2E). Thus, the ability of mutant p53 to induce PDGFRb levels is not strictly confined to a particular *p53* allele or tumor type.

We further analyzed the functional connection between mutant p53 and PDGFRb in promoting the invasiveness of human PDAC lines. Consistent with our studies in mouse PDAC lines, knockdown of either mutant p53 or PDGFRb reduced invasiveness of the A2.1 pancreatic cancer cell line (Figure 3E). Conversely, overexpression of PDGFRb in the human *p53*$^{-/-}$ ASPC pancreatic cancer cell line enhanced invasion compared to cells infected with a GFP control vector (Figure S2F). Collectively, these results confirm that upregulation of the PDGFRb receptor is important for the action of mutant p53 in PDAC and possibly other tumor types.

## Mutant p53 Disrupts the p73/NF-Y Complex to Mediate PDGFRb Expression and Tumor Cell Invasion

Several pro-oncogenic properties of mutant p53 depend on its ability to physically interact with and inhibit the p53 family members, p63 and p73 (Li and Prives, 2007). Because a previous report indicated that p73 can repress the transcription of *PDGFRB* (Hackzell et al., 2002), and because our KPC cells expressed p73, but not p63, as determined by RNA-seq (data not shown), we aimed to understand whether the physical interaction of mutant p53 with p73 might impair the ability of p73 to negatively regulate the expression of PDGFRb.

First, we verified the interaction between p73 and mutant p53 proteins by reciprocal coimmunoprecipitation (Figure 4A), and, consistent with previous reports, p73 binding to a "conformation" p53 mutant (R175H) appeared stronger than to a "DNA-binding" p53 mutant (R273H) (Gaiddon et al., 2001; Muller et al., 2009). Next, using a luciferase reporter driven from the *PDGFRB* promoter, we confirmed that overexpression of p73 in KP$_{fl}$C cells

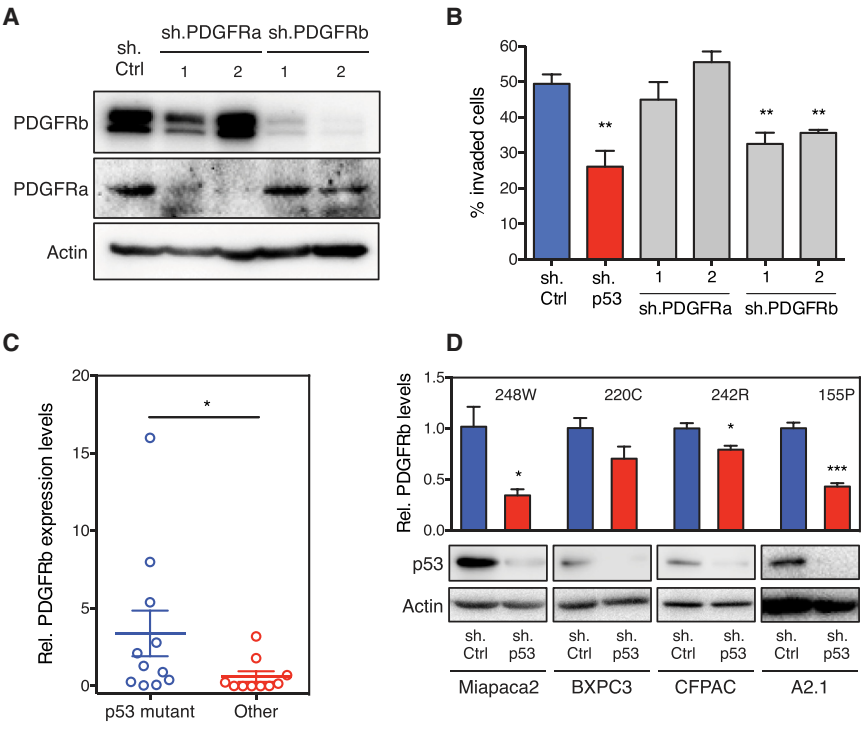


**Figure 3. Depletion of Mutant p53 in Murine and Human Pancreatic Cancer Cells Decreases PDGFRb Expression Levels to Enhance Cell Invasion**

(A) PDGFRa, PDGFRb, and actin levels of KPC cells infected with shRNAs targeting PDGFRa, PDGFRb, or a nontargeting control (Ctrl) as determined by western blotting.

(B) Quantification of the invasion into collagen of cell lines from (A), compared to KPC+sh.p53. Data presented as mean ± SD. **p < 0.005.

(C) qRT-PCR for PDGFRb in 21 human pancreatic cancer cell lines of different *p53* status. Data presented as mean normalized PDGFRb expression ± SD. *p < 0.05.

(D) qRT-PCR for PDGFRb in the human pancreatic cancer cell lines Miapaca2, BXPC3, CFPAC, and A2.1 expressing sh.p53 or sh.Ctrl. Data presented as mean normalized PDGFRb expression ± SD. *p < 0.05, ***p < 0.001. p53 mutation of each cell line as indicated. p53 and actin levels were determined by western blotting (lower panel).

(E) Quantification of invasion of human A2.1 cells infected with sh.PDGFRb, sh.p53, or sh.Ctrl (right). Data presented as mean ± SD. **p < 0.005, ***p < 0.001, ****p < 0.0001. Representative 3D reconstructions of invaded cells are shown (left).

See also Figure S2.

decreased transcriptional activity of *PDGFRB* and, conversely, that knockdown of endogenous p73 increased luciferase expression (Figures 4C and S3A). We also observed a similar increase in luciferase signal upon overexpression of two distinct forms of mutant p53 in $KP_{fl}C$ cells (Figure 4C) as well as a significant decrease upon depletion of mutant p53 or overexpression of p73 in KPC cells (Figure S3C). Importantly, depletion of endogenous p73 in KPC cells expressing mutant p53 did not enhance the transcription of *PDGFRB* (Figure S3C), indicating that the repressing activity of p73 is regulated by its interaction with mutant p53. Hence, mutant p53 cancels the ability of p73 to repress PDGFRb transcription, leading to an increase in its expression.

To better understand how p73 represses *PDGFRB* transcription, we performed chromatin immunoprecipitation (ChIP) analysis in $KP_{fl}C$ cells but failed to detect direct binding of p73 to the *PDGFRB* promoter (data not shown), a result consistent with previous reports (Matys et al., 2006). Nevertheless, promoter analysis of *PDGFRB* (Transfec, Biobase) identified a conserved CCAAT binding motif for NF-Y, a well-characterized heterotrimeric transcriptional activator (NF-YA, NF-YB, and NF-YC) of *PDGFRB*, where the NF-YB subunit interacts with p73 but is devoid of transcriptional activity (Ballagi et al., 1995; Ishisaki et al., 1997; Serra et al., 1998). We verified NF-Y binding to the *PDGFRB* promoter by use of ChIP analysis (Figure 4B). Remarkably, this binding was prevented by p73 overexpression, suggesting that the p73/NF-Y interaction hampers its ability to bind and activate the *PDGFRB* promoter (Figure 4B). Indeed, when we immunoprecipitated p73 in $KP_{fl}C$ cells, we detected direct binding of NF-YB to p73 (Figure 4A). This interaction was abrogated upon expression of mutant p53, indicating that it disrupts or interferes with the formation of the inhibitory p73/NF-Y complex (Figure 4A).

Next, we tested whether the repressive action of p73 on *PDGFRB* transcription was mediated by NF-Y and modulated by mutant p53, and we considered the implications of this regulatory circuit for invasion. Interestingly, the ability of p73 overexpression to inhibit the *PDGFRB*-luc reporter was abolished by depletion of NF-YB (Figures 4D and S3B), and NF-YB knockdown suppressed the ability of mutant p53 to enhance PDGFRb expression in $KP_{fl}C$ cells (Figure S3D). As expected, p73 overexpression reduced the invasive potential of $KP_{fl}C$ cells, whereas knockdown of p73 or overexpression of mutant p53 significantly increased invasiveness (Figure 4E). Conversely, as occurred in mutant p53 cells following p73 overexpression,

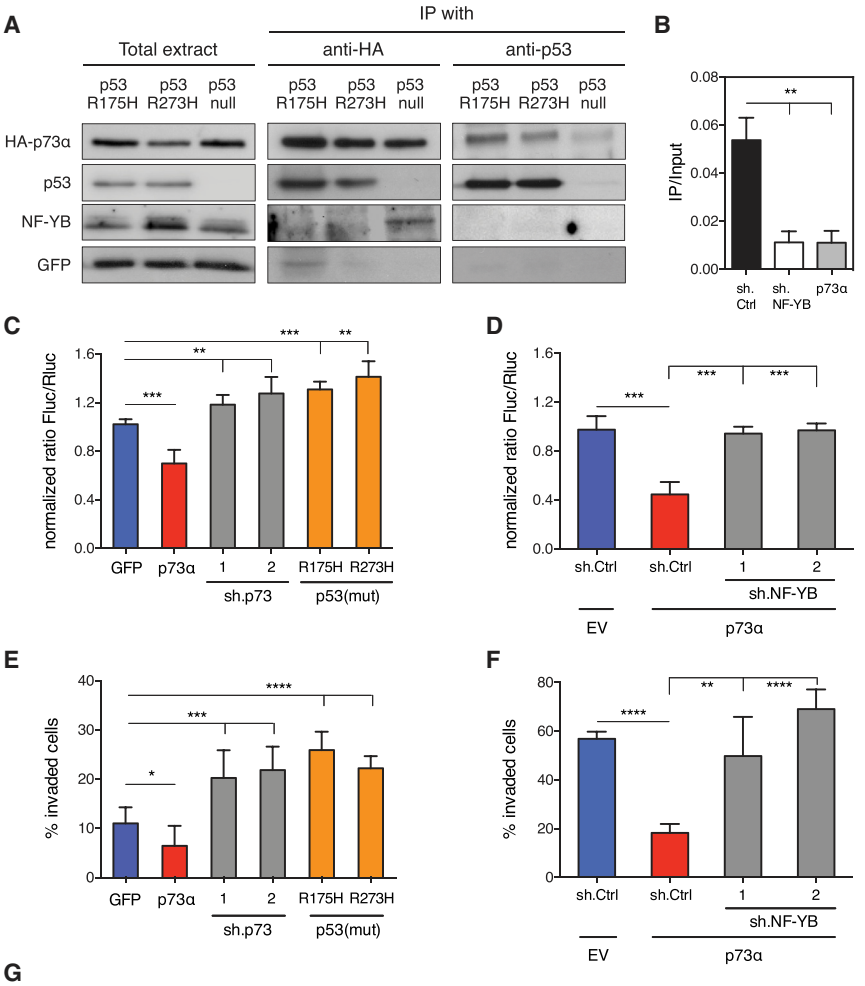


**Figure 4. Mutant p53 Sequesters p73 to Impede the Repressive Function of the p73/NF-Y Complex on the *PDGFRB* Promoter**

(A) $KP_{fl}C$ cells stably expressing a GFP, $p53^{R175H}$, or $p53^{R273H}$ vector were transfected with HA. TAp73α. Either p53 or HA was immunoprecipitated, and the expression of HAp73α, p53, or NF-YB was determined in both the input (10% of lysates) and immunoprecipitation.

(B) Chromatin immunoprecipitation (ChIP) using NF-YB antibodies in $KP_{fl}C$ cells stably expressing sh.Ctrl, sh.NF-YB, or HAp73α. Values are means ± SD. $^{**}p < 0.01$.

(C) $KP_{fl}C$ cells stably expressing a GFP, HAp73α, $p53^{R175H}$, or $p53^{R273H}$ vector or sh.p73 (1 or 2) were cotransfected with the *PDGFRB* promoter luciferase construct and renilla luciferase vector. Firefly-luciferase activity of GFP vector cells was set to one. Values are relative Firefly luciferase (Fluc) units normalized by renilla expression (Rluc) ± SD of quadruplicate samples. $^{**}p < 0.01$, $^{***}p < 0.001$. A representative result of three repeated experiments is shown.

(D) $KP_{fl}C$+GFP cells and $KP_{fl}C$+HAp73α cells superinfected with sh.Ctrl or sh.NF-YB (1 or 2) were cotransfected with the *PDGFRB* promoter luciferase construct and renilla luciferase vector. Luciferase activity was measured as described above. $^{***}p < 0.001$.

(E) Quantification of invasion of the same cells as in (C). Data presented as mean ± SD. $^{*}p < 0.05$, $^{***}p < 0.001$, $^{****}p < 0.0001$.

(F) Quantification of invasion of same cells as in (D). Data presented as mean ± SD. $^{**}p < 0.01$, $^{****}p < 0.0001$.

(G) Scheme summarizing the mechanism of action of mutant p53 in promoting invasiveness.

See also Figure S3.

depletion of p53 also reduced the invasive behavior in KPC cells (Figure S3E). Finally, NF-YB knockdown restored the invasive potential of $KP_{fl}C$ cells that overexpressed p73 (Figure 4F) and suppressed the ability of mutant p53 to enhance cell invasion (Figure S3F). Together, these results support a model in which mutant p53 promotes invasion in pancreatic cancer cells, in part, via an indirect mechanism that depends on its ability to enhance PDGFRb expression through the disruption of the inhibitory p73/NF-Y complex (Figure 4G).

## Modulation of PDGFRb Expression Levels Mediates the Phenotypic Effects of Mutant p53 Depletion In Vivo

Following the observation that p53 mutants induce the expression of PDGFRb to promote cell invasion in PDAC cultures, we investigated whether PDGFRb levels regulate metastatic behavior of PDAC cells in mice. To this end, we performed a lung colonization assay by injecting KPC+sh.p53, KPC+sh.PDGFRb, KPC+sh.PDGFRa, or KPC+sh.Ctrl cells intravenously via the tail vein into athymic mice, and then we quantified the number of colonies formed in the lungs. We found that, whereas KPC+sh.Ctrl and KPC+sh.PDGFRa cells expressing mutant p53 formed tumor nodules in the lungs at high frequency, PDGFRb depletion significantly reduced the number of lung colonies, phenocopying the antimetastatic effect observed upon knocking down mutant p53 (Figures 5A and S4A). However, depletion of PDGFRb did not affect the size of the metastatic foci, suggesting that PDGFRb does not alter their capacity to grow and proliferate in a new environment (Figure S4B). In whole-lung sections, GFP-positive signals coincided with metastatic nodules, indicating that metastases formed from cells expressing shRNAs and likely not from the proliferation of tumor cells that lost shRNA expression (Figure S4C).

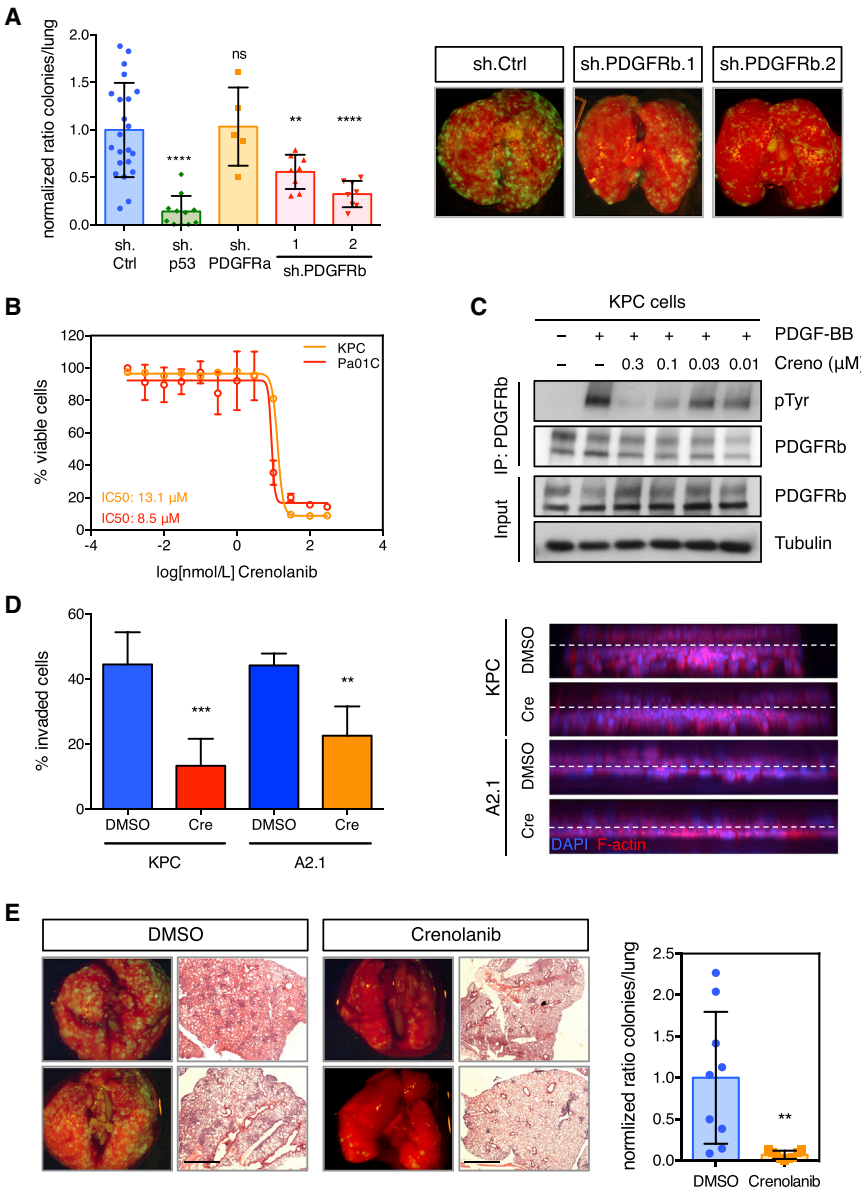


**Figure 5. PDGFRb Mediates Mutant p53 Prometastatic Function In Vivo**

(A) Lung colonization assays after tail vein injection of KPC cells +sh.PDGFRa, +sh.PDGFRb (1 or 2), +sh.p53, or +sh.Ctrl. The total number of lung metastatic nodules in individual mice ($n > 5$) was counted on serial histological sections (left). Data presented as mean ± SD. $^{**}p < 0.01$, $^{****}p < 0.0001$. Representative merged brightfield/GFP images of whole lung from indicated mice (right).

(B) MTS assay ($E_{490}$) of murine KPC and human A2.1 cells treated with crenolanib with various doses for 72 hr. Normalized values presented as mean ± SD from quadruple replicates.

(C) Immunoprecipitation of PDGFRb from KPC cells stimulated with 50 ng/ml PDGF-BB after crenolanib or DMSO treatment for 4 hr. Protein levels of PDGFRb, phospho-Tyrosine, and tubulin were determined by western blotting.

(D) Quantification of invasion of murine KPC and human A2.1 treated with either DMSO or crenolanib at 300 nM (left). Data presented as mean ± SD. $^{**}p < 0.01$, $^{***}p < 0.001$. Representative 3D reconstructions of invaded cells are shown (right).

(E) Lung colonization assays after tail vein injection of crenolanib- (300 nM) or DMSO-treated KPC cells. Representative merged brightfield/GFP imaged of whole lung and hematoxylin and eosin (H&E) stains of pulmonary lobes are shown (left). Quantification of the total number of lung metastatic nodules in individual mice ($n > 6$) (right). Data presented as mean ± SD. $^{**}p < 0.01$. Scale bars represent 1,000 μm.

See also Figure S4.

We next sought to examine whether pharmacologic inhibition of the PDGFRb pathway recapitulates the effects of PDGFRb or mutant p53 depletion (Figures 5A and S4A). We used the compound crenolanib, a small molecule inhibitor of type III tyrosine kinases, potent against PDGFRa, PDGFRb, and FLT3, but not against other known receptor tyrosine kinases (VEGFR, FGFR), serine/threonine (RAF), or tyrosine kinases (ABL1) (Lewis et al., 2009). We assessed the potency and efficacy of crenolanib on inhibiting the viability of murine KPC and human A2.1 pancreatic cancer cells and found that the dose-response patterns were comparable between the two cell lines, with $IC_{50}$ values of 13.1 and 8.5 μM, respectively (Figure 5B). Strong inhibition of PDGFRb activity, as measured by phospho-PDGFRb, was achieved in both cell lines at 0.3 μM, a dose at which no toxicity was observed (Figures 5C and S4D). Time-course experiments revealed that strong target inhibition was achieved within 10 min of drug treatment (Figure S4E). Accordingly, crenolanib treatment of KPC and A2.1 cells substantially reduced invasion relative to that seen with cells treated with DMSO (Figure 5D).

To test whether crenolanib can suppress metastasis, KPC cells were pretreated with the drug overnight and injected intravenously into recipient mice that were subsequently assessed for colony formation in the lung. Although drug treatment had no effect on the viability of the injected cell population, mice injected with drug-treated KPC cells showed significantly fewer lung nodules compared to controls pretreated with DMSO (Figures 5E and S4F). Conversely, the same concentration of crenolanib did not reduce the metastatic potential of $KP_{fl}C$ cells in a lung colonization assay, suggesting that PDGFRb acts autonomously in KPC cells to potentiate cell invasion and metastasis (Figure S4G). Further supporting this notion, conditioned media from KPC cells and most human pancreatic cell lines tested triggered PDGFRb phosphorylation in serum-starved 3T3 cells, indicating pancreatic cancer cells can provide a source of PDGF ligand that could trigger autocrine activation of PDGFRb (Figure S4H; data not shown). Therefore, abrogation of this signaling by RNAi or small

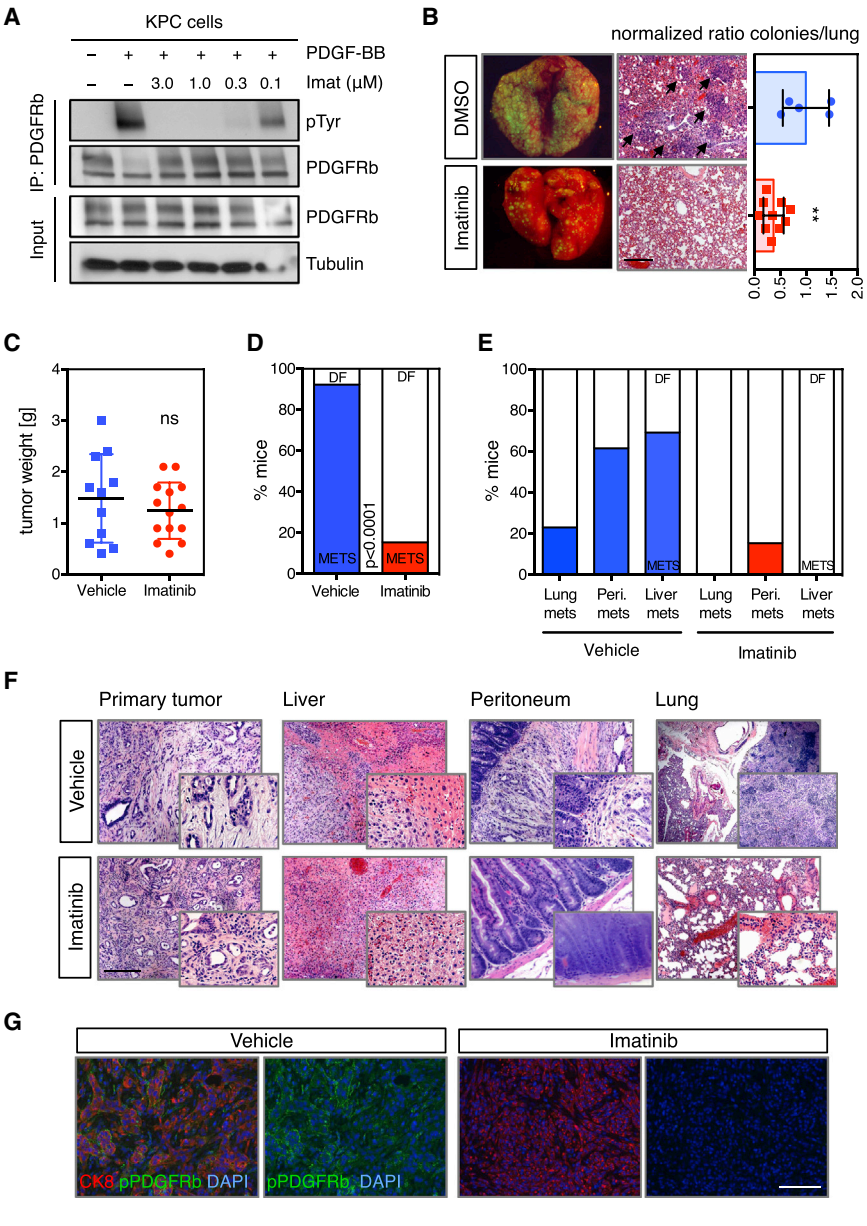


**Figure 6. Imatinib Reduces the Incidence of Metastasis in KPC Mice through PDGFRb Inhibition**

(A) Immunoprecipitation of PDGFRb from KPC cells stimulated with 50 ng/ml PDGF-BB after imatinib or DMSO treatment for 4 hr. Protein levels of PDGFRb, phospho-Tyrosine, and tubulin were determined by western blotting.

(B) Lung colonization assays after tail vein injection of imatinib- (3 μM) or DMSO-treated KPC cells. Representative merged brightfield/GFP images of whole-lung and H&E stains of pulmonary lobes are shown. Arrows indicate metastases (middle panel). Quantification of the total number of lung metastatic nodules in individual mice ($n > 5$) (right panel). Data presented as mean ± SD. $^{**}p < 0.01$. Scale bars represent 100 μm.

(C) Weight of pancreatic tumors of KPC mice treated with vehicle or imatinib at time of death.

(D) Quantification of the number of mice with metastatic disease at the time of death. Values are percentages of the total number of mice in each cohort. Colored columns represent mice with metastases (METS), and white columns represent disease-free (DF) animals.

(E) Quantification of the number of mice with lung, peritoneal (Peri.), or liver metastatic disease at the time of death. Values are percentages of the total number of mice in each cohort.

(F) Representative H&E stains of harvested organs (primary tumor, lung, liver, or peritoneal tissue) from vehicle and imatinib-treated animals. Scale bars represent 100 or 50 μm (insets).

(G) Representative immunofluorescence images of pancreatic tumors of vehicle- or imatinib-treated KPC mice. DAPI, blue; CK8, red; and pPDGFRb, green. Scale bars represent 100 μm. See also Figure S5.

molecule inhibitors leads to a significant reduction of invasion and metastasis driven by mutant p53 in vitro and in vivo.

## Imatinib Inhibits the Development of Metastases in a PDAC Mouse Model by Targeting PDGFRb

The results described above imply that pharmacologic inhibition of PDGFRb could have antimetastatic effects. We therefore sought to determine whether PDGFRb inhibition prevents metastasis in KPC mice that develop metastatic disease with a variable latency of 3 to 10 months in 50%–80% of animals (Hingorani et al., 2005). For long-term treatment of KPC mice, we decided to use FDA-approved imatinib, a potent inhibitor of PDGFRb, c-KIT, and BCR-ABL activity. Notably, the c-KIT and BCR-ABL kinases have not been linked to PDAC development (Jones et al., 2008).

Inhibition of PDGFRb by imatinib in KPC cells strongly reduced PDGFRb tyrosine phosphorylation at 3 μM (Figure 6A), a dose of the drug that is significantly lower than that required to inhibit cell proliferation ($IC_{50}$ of 29.7 μM) (Figure S5A). Nonetheless, imatinib treatment significantly reduced the invasive potential of KPC cells in vitro (Figure S5B). More importantly, pretreatment of KPC cells with imatinib decreased their potential to colonize the lungs of recipient athymic mice to a similar extent as that seen upon crenolanib treatment (Figure 6B).

We next treated KPC mice with imatinib to assess its effects on metastasis. To this end, mice were treated with a dose of 50 mg/kg imatinib by oral gavage twice daily, a regimen previously shown to produce therapeutic concentrations of imatinib in mice (Wolff et al., 2003). Treatment was initiated in mice of 8 weeks of age, a time at which KPC mice have developed preneoplastic lesions (Hingorani et al., 2005), and mice were monitored until they became symptomatic. Imatinib had no impact on tumor volume in the pancreas or overall survival, suggesting that

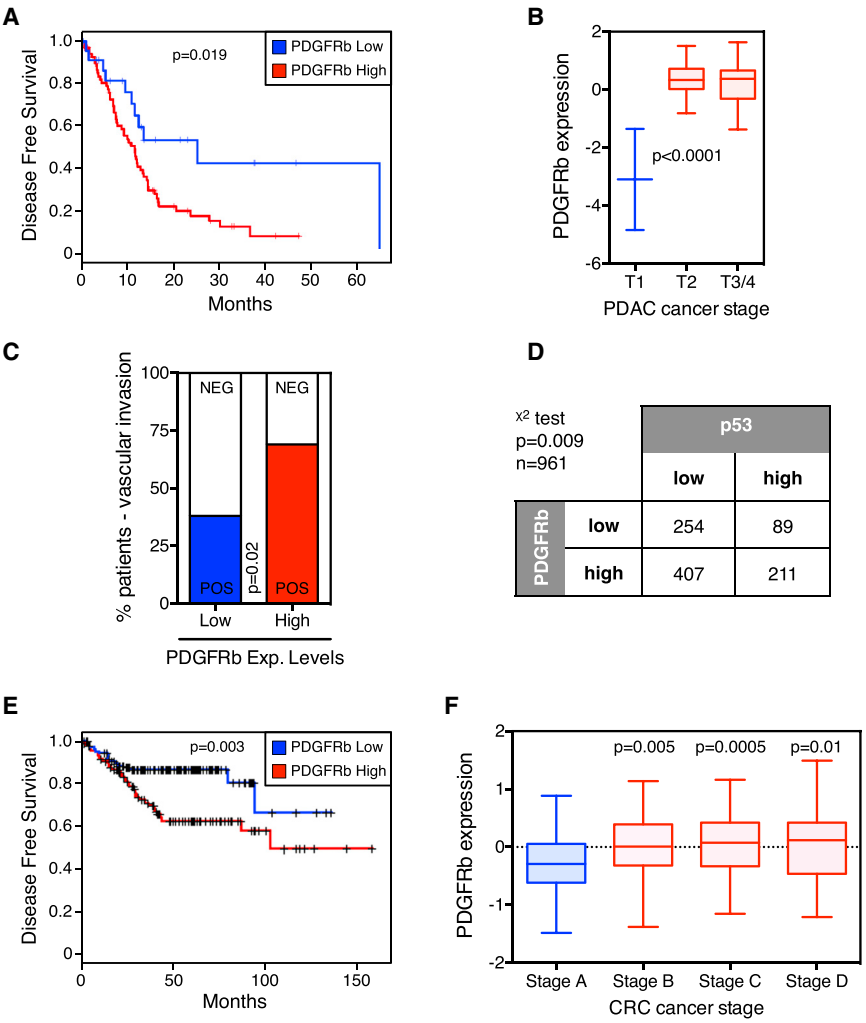


**Figure 7. High PDGFRb Expression in Human Pancreatic and Colorectal Cancer Correlates with Reduced Metastases-free Survival**

(A) Kaplan-Meier survival curves of 98 pancreatic cancer patients (clinical variable = DFS) as a function of PDGFRb-high versus PDGFRb-low expressing tumors.

(B) Box plot of PDGFRb expression versus tumor grade of pancreatic tumors (n = 98). Data presented as mean ± SD.

(C) Clinicopathologic analysis of vascular space invasion of pancreatic cancer patients stratified by the expression levels of PDGFRb in the primary tumor.

(D) Stratification of human PDAC samples (n = 961) based on high and low pPDGFRb and p53 expression levels. The chi-square test was performed (p = 0.009). p53 and pPDGFRb levels were assessed by immunofluorescence (IHC) and scored using a relative scale from 0 to 3.

(E) Kaplan-Meier survival curves of colorectal cancer patients (clinical variable = DFS) as a function of PDGFRb-high versus PDGFRb-low expressing tumors.

(F) Box plot of PDGFRb expression versus tumor grade of colon tumors (n = 290). Data presented as mean ± SD.

See also Figure S6.

the high disease burden in the pancreas was the primary cause of death (Figures 6C and S5C).

However, imatinib induced a striking reduction in the occurrence of metastasis. The incidence of metastasis was 92% in vehicle-treated animals compared to 15% in mice treated with imatinib, as assessed by macroscopic examination and confirmed by histopathological analyses ($\chi^2$ test, $p < 0.0001$) (Figures 6D and S5D). The antimetastatic effect was observed across several organs, such as liver, peritoneum, and lung (Figures 6E and 6F). As expected, imatinib was able to effectively inhibit PDGFRb activity in primary tumors based on reduced levels of phospho-PDGFRb in the tumor cells (Figures 6G and S5E). Together, these data suggest that by inhibiting the kinase activity of PDGFRb, imatinib significantly diminishes the metastatic potential of pancreatic cancer cells.

## PDGFRb Expression Correlates with Disease-free Survival in Human Pancreatic, Colorectal, and Ovarian Cancer Patients

To investigate the clinical significance of PDGFRb expression, we examined whether upregulation of this gene is correlated with prognosis or with the clinicopathological characteristics of PDACs in patients. To avoid confounding signals from the tumor stroma, PDGFRb mRNA levels were assessed in tumor samples with high purity score. Strikingly, we observed that pancreatic cancer patients with tumors expressing high levels of PDGFRb showed a poor disease-free survival and hence shorter time to relapse, including metastases in distant organs (p = 0.019) (Figure 7A). Additionally, PDGFRb expression levels were significantly elevated in late-stage PDAC as compared to the earlier stages (Figure 7B). Patients with high PDGFRb levels also displayed an increase in tumor cells invading the vascular space, another clinicopathological characteristic of tumor dissemination (Figure 7C).

Next, we tested whether PDGFRb levels correlate with the status of *p53* by analyzing a panel of PDAC tissue microarrays (TMAs). Of importance, we observed significantly higher levels of activated PDGFRb in those tumors that showed an accumulation of p53 (p = 0.009), which generally represents tumors with *p53* mutation (Oren and Rotter, 2010) (Figures 7D and S6A). These data confirmed results obtained with mice and underscore a role of mutant p53 in regulating the PDGFRb signaling in human pancreatic cancer.

Other tumor types for which *p53* mutations are predictive of metastatic disease are colorectal and ovarian cancer (Russo et al., 2005; Levesque et al., 1995). Thus, we analyzed the clinical significance of PDGFRb in these cancer types and found that levels of PDGFRb significantly stratified colorectal and ovarian

tumor patients into two distinct cohorts. Patients with tumors expressing low PDGFRb levels exhibit a lower probability to form metastases compared to patients with PDGFRb high-expressing tumors ($p = 0.003$ and $p < 0.0001$) (Figures 7E and S6C). As in PDAC, a significant increase in PDGFRb expression was observed in higher-stage colorectal cancers (Figure 7F). In addition to PDGFRb, our mutant *p53* gene signature significantly scored as a prognostic marker in colorectal and ovarian tumor patients (top 40 genes upregulated in KPC cells; Figure 2C; Table S1). When we analyzed the three genes that scored in our invasion assay screen, we found that the *PDGFRB* gene was the strongest predictor for the probability to develop metastasis in colorectal and ovarian cancer patients (Figures S6B and S6C). In summary, consistent with our functional studies, elevated PDGFRb expression correlated significantly with the status of p53, higher tumor stage, and a poorer disease-free survival rate in pancreatic, colorectal, and ovarian cancer patients.

## DISCUSSION

Mutations that occur in the *p53* tumor suppressor inactivate wild-type p53 functions but can also produce "gain-of-function" oncogenic properties that can contribute to cell proliferation, survival, and metastasis. Here, we explored the phenotypic effects of mutant p53 in pancreatic cancer and showed that the sustained expression of the mutant *p53* allele is necessary to maintain the invasive phenotype of PDAC cells by increasing the expression of PDGFRb. These results have several ramifications for our understanding of mutant p53 action as well as the behavior and potential treatment of pancreatic cancer.

Signaling through PDGFRb contributes to multiple tumor-associated processes, including cell invasion and metastasis. Given the generally restricted expression of PDGFRb to mesenchymal cell types, most of the oncogenic properties of PDGFRb are thought to reflect paracrine effects of tumor cell-secreted PDGF. Indeed, previous work on the role of PDGFRb in carcinoma progression and metastasis suggests that PDGFRb mainly elicits responses in the tumor stroma by promoting tumor angiogenesis (Pietras et al., 2003; Cao et al., 2004). In contrast, our study provides evidence for tumor cell-specific expression of PDGFRb in promoting metastasis. We show that genetic or pharmacological inhibition of PDGFRb in the pancreatic cancer cells themselves dramatically reduces their invasive and metastatic potential and that treatment of mice harboring genetic and histologically relevant tumors prevents metastatic spread in vivo. Together, our data indicate that pancreatic tumor cells expressing mutant p53 not only synthesize PDGF but also upregulate PDGFRb, leading to a tumor autocrine, cell-autonomous effect.

Though increases in PDGFRb expression were necessary and sufficient to mediate mutant p53 effects in our model, we identified at least two additional genes (*SNED1* and *SLC40A1*) that also contribute to the invasive phenotype through yet unknown mechanisms. Studies in other systems, primarily breast cancer, have suggested that CXCR4, cyclin-G2, and the mevalonate pathway are important mediators of the prometastatic activities of mutant p53 (Mehta et al., 2007; Adorno et al., 2009; Freed-Pastor et al., 2012). In addition, mutant p53 has also been reported to drive invasion by regulating several miRNAs, such as miR155 and miR130b (Neilsen et al., 2013; Dong et al., 2013). In agreement, we found that miR155 is positively regulated by mutant p53 in KPC cells and can promote metastasis in our model (data not shown); however, in contrast to a previous report (Su et al., 2010), no effects on DICER expression were observed, arguing that in pancreatic cancer the mutant p53-associated changes in microRNA expression and metastasis are DICER independent. Additionally, miR34a expression levels were not dependent on p53 status in our system (data not shown), even though this miRNA acts as negative regulator of PDGFRb in lung cancer (Garofalo et al., 2013). Regardless, as for wild-type p53, mutant p53 exerts effects through the regulation of multiple genes rather than by modulating a single signaling pathway.

Most of our understanding of how mutant p53 mediates its oncogenic activity has been derived from exploring the consequences of the physical interaction between the mutant protein and the p53 family members, p63 and p73. Whereas the mutant p53-p63 interaction modulates the expression of p63 target genes to enhance invasion and metastasis (Adorno et al., 2009; Muller et al., 2009), how p53-p73 interactions produce similar outcomes is poorly understood. Here, we show that mutant p53 enhances pancreatic cancer cell metastasis by modulating p73 and its interaction with the transcriptional activator NF-Y. This model is consistent with previous studies showing that (1) loss of p73 in a *p53* null background might be functionally equivalent to the expression of mutant p53 (Lang et al., 2004); (2) aberrant transcriptional regulation by mutant p53 is mediated through the transcriptional activator NF-Y (Di Agostino et al., 2006); and (3) mutant p53 promotes recycling of receptor tyrosine kinases to initiate invasion (Muller et al., 2009). Whether structurally distinct p53 mutants enhance metastasis to the same extent and through the same mechanism remains unclear, and certainly most truncating mutants arising from the nonsense mutations occurring in a fraction of pancreas cancers are predicted to behave as if *p53* null. Still, in our study both conformational (e.g., R175H) and structural mutants (e.g., R273H) were capable of inducing *PDGFRB* through a similar mechanism.

Questions remain as to how the mutant p53/p73/NF-Y regulatory axis acts mechanistically. For instance, it remains unclear whether p73 acts to suppress the transactivation capacity of NF-Y or whether it sequesters the activator and prevents its binding to the *PDGFRB* promoter. Even though our results indicate that p73 overexpression hampers the ability of NF-Y to bind to the *PDGFRB* promoter, further studies will be required to distinguish between mechanisms. In addition, we noted slightly stronger induction of *PDGFRB* transcription as well as higher levels of invasion upon overexpression of mutant p53 compared to depletion of p73, indicating that mutant p53 may exert additional regulatory effects on PDGFRb expression. Although studies suggest that mutant p53 can directly bind to NF-Y to regulate its transcriptional activity (Di Agostino et al., 2006), we failed to observe any physical interaction between mutant p53 and NF-Y in our cells. The discrepancy could reflect different extraction conditions or biological settings, because the mutant p53/NF-Y interaction has been shown to occur upon DNA damage (Liu et al., 2011).

Mutations in *KRAS*, *p53*, *CDKN2A*, *BRCA2*, and *SMAD4* define the genetic landscape of PDAC; however, it remains unclear how each mutation contributes to the malignant evolution of this aggressive disease. We present evidence for a crucial role of mutant p53 in metastasis formation, which supports the attractive concept of targeting its gain-of-function activities to limit cancer cell dissemination and metastasis. However, mutant p53 is neither a targetable cell-surface protein nor a druggable enzyme (Levine and Oren, 2009), and novel therapeutic modalities, such as RNAi or restoring wild-type p53 conformations, have yet to show efficacy in clinical studies (Lehmann and Pietenpol, 2012). Hence, targeting downstream pathways or genes that mediate the activity of mutant p53, such as PDGFRb, pose an alternative treatment strategy.

Owing to the early metastatic spread of pancreatic cancer, widespread use of PDGFRb inhibitors might require advances in early detection or combination with other therapies. Nonetheless, our study suggests that PDGFRb inhibition might prove immediately useful in pancreatic patients harboring *p53* missense mutations either before (neoadjuvant) or after surgical resection (adjuvant) of localized disease (10%–15% of PDAC cases), in patients with locally advanced inoperable nonmetastatic disease (~30% of PDAC cases) or as a preventative approach in patients with familial predisposition to cancer development. Moreover, PDGFRb inhibition as a therapeutic approach could be extended to other metastatic cancer types, e.g., colorectal, where the disease is often diagnosed before tumor cell dissemination.

High levels of PDGFRb expression have recently been associated with tumor recurrence in primary colorectal cancer, another gastrointestinal tumor in which *p53* is frequently mutated (Steller et al., 2013). Accordingly, we noted correlations between elevated PDGFRb levels, more-advanced tumor stage, and poorer disease-free survival in pancreatic, as well as colorectal and ovarian, cancer patients. These results indicate that PDGFRb levels might be used as a prognostic biomarker for cancer progression and eventually be used in conjunction with p53 to identify patient cohorts most likely to respond to therapies targeting this axis. Although further studies will be required to explore this notion, pharmacological inhibition of PDGFRb with the tyrosine kinase inhibitor imatinib, in combination with standard chemotherapy, has shown promise in treating metastatic colorectal cancer patients (Hoehler et al., 2013).

In summary, we describe a gain-of-function activity of mutant p53 that promotes invasion and metastasis through increasing *PDGFRB* transcription and reverting the repressive function of the p73/NF-Y complex. While other activities of mutant p53 on cell behavior and survival exist (Freed-Pastor and Prives, 2012), our study provides a detailed molecular understanding of at least one aspect of the invasive behavior of cells expressing mutant p53 and offers a potential target for therapy that might interfere with this activity.

## EXPERIMENTAL PROCEDURES

### Wound Healing and Invasion Assays

Wound healing and three-dimensional invasion assays were conducted as previously described (Goulimari et al., 2005; Kitzing et al., 2007). In brief, invasion assays were carried out in 24-well transwell inserts, lined with collagen type 1, and cells were seeded on the inverted inserts.

### Immunostaining and Microscopy

Invasion assay inserts were fixed using 4% formaldehyde before confocal microscopy (PerkinElmer Spinning Disk) was conducted. Images were analyzed using Imaris software.

### qRT-PCR

Real-time PCR was carried out in triplicate using SYBR Green PCR Master Mix on the ViiA 7 Real-Time PCR System.

### RNA Sequencing and Data Analysis

Directional (stranded) libraries for paired-end sequencing of KPC cells were conducted on the Illumina platform. Differential expression analysis for sequence count data (fragments per kilobase of transcript per million mapped reads [FPKM] values) was conducted using DESeq.

### PDGFRb Luciferase Reporter Assay

Cells were transiently transfected with expression plasmid, reporter plasmid, and renilla luciferase vector. After 36 hr, firefly luciferase and renilla activities were measured on a Varioskan Flash Multimode Reader.

### Chromatin Immunoprecipitation

Chromatin immunoprecipitation was performed as previously described (Beckerman et al. 2009). In brief, Protein A/G Sepharose beads conjugated to anti-NF-YB antibody were used to immunoprecipitate NF-YB from whole cell lysates. Quantitative ChIP was carried out on an ABI StepOne Plus using SYBR green dye.

### Mouse Studies

All animal experiments were performed in accordance with a protocol approved by the Memorial Sloan-Kettering Institutional Animal Care and Use Committee.

### Human Data Sets

Gene expression data and survival analyses of ovarian, colorectal, and pancreatic cancer patients with annotated clinical outcomes were downloaded from the Gene Expression Omnibus database (GSE50827, GSE9899, GSE17537, and GSE28735). For survival analyses, gene expression data were clustered into groups using kmeans, and Kaplan-Meier analyses was performed. Significance for these plots was determined using the log rank test.

For further details, please refer to the Extended Experimental Procedures.

## ACCESSION NUMBERS

The Sequence Read Archive (SRA) accession number of the RNA sequencing data reported in this paper is SRP033333.

## SUPPLEMENTAL INFORMATION

Supplemental Information includes Extended Experimental Procedures, six figures, and one table and can be found with this article online at http://dx.doi.org/10.1016/j.cell.2014.01.066.

## AUTHOR CONTRIBUTIONS

S.W. and E.M. designed and performed the majority of the experiments and contributed equally to this work. M.S., J.P.M., D.F.T., and T.K. contributed intellectually to the design of the project and helped perform experiments (treatment of KPC mice, IHC/immunofluorescence, TMAs, and invasion assay, respectively). E.W. and C.A.D. conducted and analyzed RNA sequencing. S.-H.M., N.T.P., and C. Prives conducted and analyzed ChIP experiments. E.K.M., J.W., S.M.G., and A.V.B. collected, analyzed, and interpreted human data. C. Pilarsky and D.A. provided TMAs and their p53 status.

S.W., E.M., and S.W.L. wrote the manuscript with assistance from all authors. S.W.L. conceived and supervised the project.

## ACKNOWLEDGMENTS

We thank K. Funa for sharing plasmids, A. Lujambio, M. Taylor, J. Ahn, and other members of the Lowe laboratory for critical discussions and/or technical help, APGI for providing clinical data, and J.P. Morton for providing cell lines. We thank C.J. Sherr and L. Dow for their advice on experimental design and for editing the manuscript. S.W. is the recipient of the Annette Kade Fellowship from the Watson School of Biological Sciences. E.M. is supported by The Jane Coffin Childs Memorial Fund for Medical Research. S.W.L. is the Geoffrey Beene Chair of Cancer Biology and a Howard Hughes Medical Institute investigator. This work was supported by a grant from the National Cancer Institute (CA 013106).

Received: November 12, 2013
Revised: December 17, 2013
Accepted: January 23, 2014
Published: April 10, 2014

## REFERENCES

Adorno, M., Cordenonsi, M., Montagner, M., Dupont, S., Wong, C., Hann, B., Solari, A., Bobisse, S., Rondina, M.B., Guzzardo, V., et al. (2009). A mutant-p53/Smad complex opposes p63 to empower TGFbeta-induced metastasis. Cell *137*, 87–98.

Ballagi, A.E., Ishizaki, A., Nehlin, J.O., and Funa, K. (1995). Isolation and characterization of the mouse PDGF beta-receptor promoter. Biochem. Biophys. Res. Commun. *210*, 165–173.

Beckerman, R., Donner, A.J., Mattia, M., Peart, M.J., Manley, J.L., Espinosa, J.M., and Prives, C. (2009). A role for Chk1 in blocking transcriptional elongation of p21 RNA during the S-phase checkpoint. Genes Dev. *23*, 1364–1377.

Cao, R., Björndahl, M.A., Religa, P., Clasper, S., Garvin, S., Galter, D., Meister, B., Ikomi, F., Tritsaris, K., Dissing, S., et al. (2004). PDGF-BB induces intratumoral lymphangiogenesis and promotes lymphatic metastasis. Cancer Cell *6*, 333–345.

Dai, Y. (2010). Platelet-derived growth factor receptor tyrosine kinase inhibitors: a review of the recent patent literature. Expert Opin. Ther. Pat. *20*, 885–897.

Di Agostino, S., Strano, S., Emiliozzi, V., Zerbini, V., Mottolese, M., Sacchi, A., Blandino, G., and Piaggio, G. (2006). Gain of function of mutant p53: the mutant p53/NF-Y protein complex reveals an aberrant transcriptional mechanism of cell cycle regulation. Cancer Cell *10*, 191–202.

Dong, P., Karaayvaz, M., Jia, N., Kaneuchi, M., Hamada, J., Watari, H., Sudo, S., Ju, J., and Sakuragi, N. (2013). Mutant p53 gain-of-function induces epithelial-mesenchymal transition through modulation of the miR-130b-ZEB1 axis. Oncogene *32*, 3286–3295.

Freed-Pastor, W.A., and Prives, C. (2012). Mutant p53: one name, many proteins. Genes Dev. *26*, 1268–1286.

Freed-Pastor, W.A., Mizuno, H., Zhao, X., Langerød, A., Moon, S.H., Rodriguez-Barrueco, R., Barsotti, A., Chicas, A., Li, W., Polotskaia, A., et al. (2012). Mutant p53 disrupts mammary tissue architecture via the mevalonate pathway. Cell *148*, 244–258.

Gaiddon, C., Lokshin, M., Ahn, J., Zhang, T., and Prives, C. (2001). A subset of tumor-derived mutant forms of p53 down-regulate p63 and p73 through a direct interaction with the p53 core domain. Mol. Cell. Biol. *21*, 1874–1887.

Garofalo, M., Jeon, Y.J., Nuovo, G.J., Middleton, J., Secchiero, P., Joshi, P., Alder, H., Nazaryan, N., Di Leva, G., Romano, G., et al. (2013). MiR-34a/c-dependent PDGFR-$\alpha$/$\beta$ downregulation inhibits tumorigenesis and enhances TRAIL-induced apoptosis in lung cancer. PLoS ONE *8*, e67581.

Goulimari, P., Kitzing, T.M., Knieling, H., Brandt, D.T., Offermanns, S., and Grosse, R. (2005). Galpha12/13 is essential for directed cell migration and localized Rho-Dia1 function. J. Biol. Chem. *280*, 42242–42251.

Hackzell, A., Uramoto, H., Izumi, H., Kohno, K., and Funa, K. (2002). p73 independent of c-Myc represses transcription of platelet-derived growth factor beta-receptor through interaction with NF-Y. J. Biol. Chem. *277*, 39769–39776.

Hanel, W., Marchenko, N., Xu, S., Yu, S.X., Weng, W., and Moll, U. (2013). Two hot spot mutant p53 mouse models display differential gain of function in tumorigenesis. Cell Death Differ. *20*, 898–909.

Hidalgo, M. (2010). Pancreatic cancer. N. Engl. J. Med. *362*, 1605–1617.

Hingorani, S.R., Petricoin, E.F., Maitra, A., Rajapakse, V., King, C., Jacobetz, M.A., Ross, S., Conrads, T.P., Veenstra, T.D., Hitt, B.A., et al. (2003). Preinvasive and invasive ductal pancreatic cancer and its early detection in the mouse. Cancer Cell *4*, 437–450.

Hingorani, S.R., Wang, L., Multani, A.S., Combs, C., Deramaudt, T.B., Hruban, R.H., Rustgi, A.K., Chang, S., and Tuveson, D.A. (2005). Trp53R172H and KrasG12D cooperate to promote chromosomal instability and widely metastatic pancreatic ductal adenocarcinoma in mice. Cancer Cell *7*, 469–483.

Hoehler, T., von Wichert, G., Schimanski, C., Kanzler, S., Moehler, M.H., Hinke, A., Seufferlein, T., Siebler, J., Hochhaus, A., Arnold, D., et al. (2013). Phase I/II trial of capecitabine and oxaliplatin in combination with bevacizumab and imatinib in patients with metastatic colorectal cancer: AIO KRK 0205. Br. J. Cancer *109*, 1408–1413.

Ishisaki, A., Murayama, T., Ballagi, A.E., and Funa, K. (1997). Nuclear factor Y controls the basal transcription activity of the mouse platelet-derived-growth-factor beta-receptor gene. Eur. J. Biochem. *246*, 142–146.

Joerger, A.C., and Fersht, A.R. (2007). Structural biology of the tumor suppressor p53 and cancer-associated mutants. Adv. Cancer Res. *97*, 1–23.

Jones, S., Zhang, X., Parsons, D.W., Lin, J.C., Leary, R.J., Angenendt, P., Mankoo, P., Carter, H., Kamiyama, H., Jimeno, A., et al. (2008). Core signaling pathways in human pancreatic cancers revealed by global genomic analyses. Science *321*, 1801–1806.

Kitzing, T.M., Sahadevan, A.S., Brandt, D.T., Knieling, H., Hannemann, S., Fackler, O.T., Grosshans, J., and Grosse, R. (2007). Positive feedback between Dia1, LARG, and RhoA regulates cell morphology and invasion. Genes Dev. *21*, 1478–1483.

Lang, G.A., Iwakuma, T., Suh, Y.A., Liu, G., Rao, V.A., Parant, J.M., Valentin-Vega, Y.A., Terzian, T., Caldwell, L.C., Strong, L.C., et al. (2004). Gain of function of a p53 hot spot mutation in a mouse model of Li-Fraumeni syndrome. Cell *119*, 861–872.

Lehmann, B.D., and Pietenpol, J.A. (2012). Targeting mutant p53 in human tumors. J. Clin. Oncol. *30*, 3648–3650.

Levesque, M.A., Katsaros, D., Yu, H., Zola, P., Sismondi, P., Giardina, G., and Diamandis, E.P. (1995). Mutant p53 protein overexpression is associated with poor outcome in patients with well or moderately differentiated ovarian carcinoma. Cancer *75*, 1327–1338.

Levine, A.J., and Oren, M. (2009). The first 30 years of p53: growing ever more complex. Nat. Rev. Cancer *9*, 749–758.

Lewis, N.L., Lewis, L.D., Eder, J.P., Reddy, N.J., Guo, F., Pierce, K.J., Olszanski, A.J., and Cohen, R.B. (2009). Phase I study of the safety, tolerability, and pharmacokinetics of oral CP-868,596, a highly specific platelet-derived growth factor receptor tyrosine kinase inhibitor in patients with advanced cancers. J. Clin. Oncol. *27*, 5262–5269.

Li, Y., and Prives, C. (2007). Are interactions with p63 and p73 involved in mutant p53 gain of oncogenic function? Oncogene *26*, 2220–2225.

Li, D., Xie, K., Wolff, R., and Abbruzzese, J.L. (2004). Pancreatic cancer. Lancet *363*, 1049–1057.

Liu, K., Ling, S., and Lin, W.C. (2011). TopBP1 mediates mutant p53 gain of function through NF-Y and p63/p73. Mol. Cell. Biol. *31*, 4464–4481.

Longati, P., Jia, X., Eimer, J., Wagman, A., Witt, M.R., Rehnmark, S., Verbeke, C., Toftgård, R., Löhr, M., and Heuchel, R.L. (2013). 3D pancreatic carcinoma spheroids induce a matrix-rich, chemoresistant phenotype offering a better model for drug testing. BMC Cancer *13*, 95.

Masciarelli, S., Fontemaggi, G., Di Agostino, S., Donzelli, S., Carcarino, E., Strano, S., and Blandino, G. (2013). Gain-of-function mutant p53

downregulates miR-223 contributing to chemoresistance of cultured tumor cells. Oncogene. Published online April 15, 2013. http://dx.doi.org/10.1038/onc.2013.106.

Matys, V., Kel-Margoulis, O.V., Fricke, E., Liebich, I., Land, S., Barre-Dirrie, A., Reuter, I., Chekmenev, D., Krull, M., Hornischer, K., et al. (2006). TRANSFAC and its module TRANSCompel: transcriptional gene regulation in eukaryotes. Nucleic Acids Res. *34* (Database issue), D108–D110.

Mehta, S.A., Christopherson, K.W., Bhat-Nakshatri, P., Goulet, R.J., Jr., Broxmeyer, H.E., Kopelovich, L., and Nakshatri, H. (2007). Negative regulation of chemokine receptor CXCR4 by tumor suppressor p53 in breast cancer cells: implications of p53 mutation or isoform expression on breast cancer cell invasion. Oncogene *26*, 3329–3337.

Montalbetti, N., Simonin, A., Kovacs, G., and Hediger, M.A. (2013). Mammalian iron transporters: families SLC11 and SLC40. Mol. Aspects Med. *34*, 270–287.

Morton, J.P., Timpson, P., Karim, S.A., Ridgway, R.A., Athineos, D., Doyle, B., Jamieson, N.B., Oien, K.A., Lowy, A.M., Brunton, V.G., et al. (2010). Mutant p53 drives metastasis and overcomes growth arrest/senescence in pancreatic cancer. Proc. Natl. Acad. Sci. USA *107*, 246–251.

Muller, P.A., Caswell, P.T., Doyle, B., Iwanicki, M.P., Tan, E.H., Karim, S., Lukashchuk, N., Gillespie, D.A., Ludwig, R.L., Gosselin, P., et al. (2009). Mutant p53 drives invasion by promoting integrin recycling. Cell *139*, 1327–1341.

Neilsen, P.M., Noll, J.E., Mattiske, S., Bracken, C.P., Gregory, P.A., Schulz, R.B., Lim, S.P., Kumar, R., Suetani, R.J., Goodall, G.J., and Callen, D.F. (2013). Mutant p53 drives invasion in breast tumors through up-regulation of miR-155. Oncogene *32*, 2992–3000.

Olive, K.P., Tuveson, D.A., Ruhe, Z.C., Yin, B., Willis, N.A., Bronson, R.T., Crowley, D., and Jacks, T. (2004). Mutant p53 gain of function in two mouse models of Li-Fraumeni syndrome. Cell *119*, 847–860.

Oren, M., and Rotter, V. (2010). Mutant p53 gain-of-function in cancer. Cold Spring Harb. Perspect. Biol. *2*, a001107.

Pietras, K., Sjöblom, T., Rubin, K., Heldin, C.H., and Ostman, A. (2003). PDGF receptors as cancer drug targets. Cancer Cell *3*, 439–443.

Russo, A., Bazan, V., Iacopetta, B., Kerr, D., Soussi, T., and Gebbia, N.; TP53-CRC Collaborative Study Group (2005). The TP53 colorectal cancer international collaborative study on the prognostic and predictive significance of p53 mutation: influence of tumor site, type of mutation, and adjuvant treatment. J. Clin. Oncol. *23*, 7518–7528.

Serra, E., Zemzoumi, K., di Silvio, A., Mantovani, R., Lardans, V., and Dissous, C. (1998). Conservation and divergence of NF-Y transcriptional activation function. Nucleic Acids Res. *26*, 3800–3805.

Soussi, T., and Béroud, C. (2001). Assessing TP53 status in human tumours to evaluate clinical outcome. Nat. Rev. Cancer *1*, 233–240.

Steller, E.J., Raats, D.A., Koster, J., Rutten, B., Govaert, K.M., Emmink, B.L., Snoeren, N., van Hooff, S.R., Holstege, F.C., Maas, C., Borel Rinkes, I.H., and Kranenburg, O. (2013). PDGFRB promotes liver metastasis formation of mesenchymal-like colorectal tumor cells. Neoplasia *15*, 204–217.

Su, X., Chakravarti, D., Cho, M.S., Liu, L., Gi, Y.J., Lin, Y.L., Leung, M.L., El-Naggar, A., Creighton, C.J., Suraokar, M.B., et al. (2010). TAp63 suppresses metastasis through coordinate regulation of Dicer and miRNAs. Nature *467*, 986–990.

Wolff, N.C., Richardson, J.A., Egorin, M., and Ilaria, R.L., Jr. (2003). The CNS is a sanctuary for leukemic cells in mice receiving imatinib mesylate for Bcr/Abl-induced leukemia. Blood *101*, 5010–5013.

Cell

## EXTENDED EXPERIMENTAL PROCEDURES

### Retroviral Constructs, Antibodies, and Reagents

All vectors were derived from the Murine Stem Cell Virus (MSCV, Clontech) retroviral vector backbone. PDGFRb cDNA (Addgene, #23893) was subcloned into MSCV-PGK-Puro-IRES-GFP (MSCV-PIG) (Hemann et al., 2003). miR30-based shRNAs were designed and cloned as previously described (Zuber et al., 2011) and sequences are available upon request. shRNAs were cloned in the MLP vector (MSCV-mir30-PGK-Puro-IRES-GFP) for constitutive expression and inducible shRNAs were cloned into the TRMPV-Neo vector (pSIN-TRE-dsRed-miR30-PGK-Venus-IRES-NeoR) as previously described (Zuber et al., 2011). All constructs were verified by sequencing.

p53 was detected using mAb NCL-P53-505 (Novocastra) and hAB OP43 (Calbiochem). Anti-Actin (A3854) was purchased from Sigma. Anti-PDGFRa (3164) and –PDGFRb (3169) antibodies were purchased from Cell Signaling. Alexa Fluor 568-Phalloidin (A12380) was purchased from Invitrogen. Crenolanib (CP-868596) and imatinib (I-5508) were purchased from Selleckchem and LC Laboratories, respectively.

### Cell Culture and Drug Treatments

All cell lines were maintained in DMEM + 10% FBS, at 37°C in 5% $CO_2$. Stable cell lines expressing shRNAs were generated by retroviral mediated gene transfer. Briefly, Phoenix-Eco and Phoenix-Ampho packaging cells (for murine or human cell lines, respectively) were transfected by the calcium phosphate method with vectors expressing NF-YA, NF-YB, p53, p73, PDGFRa, PDGFRb or Renilla-control shRNAs, and the generated viruses were harvested to infect KPC, $KP_{fl}C$, or a series of human pancreatic, breast, lung and colon cancer cell lines. Infected cells were selected with puromycin and experiments were carried out on derived cell populations. To generate cells stably expressing mutant p53, p73 or PDGFRb, $KP_{fl}C$ cells were infected with MSCV-p53-R175H, -R273H, PDGFRb or pcDNA3-HA-p73α and selected in puromycin and G418 respectively to yield stable pools. Cultured cells were treated with 300 nm crenolanib and 3 μM imatinib. These concentrations were selected after determining the concentration required to fully inhibit the phosphorylation of PDGFRb without any effects on cell proliferation.

### Wound Healing and Invasion Assays

Wound healing assays were conducted as previously described (Goulimari et al., 2005). Briefly, cells were seeded in 6-well plates, grown until confluent, and wounding was performed with a 10-μl microtiter tip that was cut longitudinally. Three-dimensional invasion assays were carried out as previously described (Kitzing et al., 2007). In brief, 24-well transwell inserts (Greiner bio-one) were lined with collagen type 1 (BD Biosciences), and cells were seeded on the inverted inserts. The lower chambers were filled with medium containing 0.5% FBS and upper chambers containing the collagen matrix were filled with medium containing 20% FBS and the chemoattractant HGF.

### Immunostaining and Microscopy

Live cell recordings were performed immediately after wounding for 18 hr at 37°C using a Zeiss observer Microscope. Pictures were acquired every 10 min with a motor-controlled Leica DC 350 FX camera, which enables simultaneous recordings from multiple wells. For statistical analysis, the wound distance from each well was measured in duplicate at three randomly defined wound gap locations per frame recorded per experiment. Invasion assay inserts were fixed using 4% formaldehyde and stained using DAPI and Alexa568 phalloidin (Invitrogen) before confocal microscopy (Perkin Elmer Spinning Disk) was conducted. Images were analyzed using Imaris software.

### qRT-PCR

Total RNA was isolated using TRIZOL (Invitrogen), and cDNA was obtained using the TaqMan reverse transcription reagents (Applied Biosystems). Real-time PCR was carried out in triplicate using SYBR Green PCR Master Mix (Applied Biosystems) on the ViiA 7 Real-Time PCR System (Invitrogen). GAPDH or β-actin served as endogenous normalization controls.

### RNA Sequencing and Data Analysis

Nucleotide sequencing of RNAs of > 200 nt length was carried out us previously described (Djebali et al., 2012). Directional (stranded) libraries for Paired End (PE) sequencing on the Illumina platform were generated as described previously (Parkhomchuk et al., 2009). Primary data processing and library mapping was completed using the Spliced Transcripts Alignment to a Reference (STAR) software (Dobin et al., 2013). Differential expression analysis for sequence count data (FPKM values) was conducted using DESeq as described previously (Anders and Huber, 2010).

### PDGFRb Luciferase Reporter Assay

The promoter assay was performed as previously described (Hackzell et al., 2002). In brief, cells were seeded in 24-well plates and transiently transfected with 0.5 ug of expression plasmid, 2.0 ug of reporter plasmid, and 20 ng of renilla-luciferase vector (PGL4.74, Promega). After 36 hr, cells were lysed (Dual-Luciferase Reporter Assay System, Promega), and firefly luciferase and renilla luciferase

activities were measured (Varioskan Flash Multimode Reader, Thermo Scientific). Results shown were normalized to renilla activity and are representative of at least three independent replicates.

### Coimmunoprecipitation

To detect p53/p73 and p73/NF-Y binding, sub-confluent $KP_{fl}C$ cells were infected with mutant p53 or an empty control construct and transiently transfected with HA.p73 (Addgene) using Lipofectamine 2000 (Invitrogen). Thirty-six hours post-transfection, cells were lysed in RIPA Buffer (20 mM Tris pH 7.4, 1% Triton X-100, 37 mM NaCl, 2 mM EDTA, 1% SDS, 0.5% NP-40, 10% Glycerol, phosphatase inhibitors [2.5 mM Sodium pyrophosphate, 1 mM β-Glycerophosphate, 1 mM $Na_3VO_4$], and protease inhibitors [Roche]). Whole cell lysates (0.5 mg protein) were pre-cleared with A/G Sepharose beads (Invitrogen), incubated at 4°C with either anti-HA (Covance, 16B12) or anti-p53 antibody (Calbiochem, OP43) overnight and subsequently with protein A/G beads for 2 hr. The bead pellet was extensively washed in lysis buffer three times and then electrophoresed on 10% SDS-PAGE gels followed by immunoblotting using anti-p53, anti-HA, anti-GFP (Cell Signaling, 2555) and anti-NF-YB (Santa Cruz, FL-207) antibodies.

To measure levels of endogenously phosphorylated PDGFRb, KPC cells were treated with the drug as described and harvested in phospho-lysis buffer (50 mM Tris pH 7.5, 1% Tween-20, 200 mM NaCl, 0.2% NP-40, phosphatase inhibitors [2.5 mM Sodium pyrophosphate, 1 mM β-Glycerophosphate, 1 mM $Na_3VO_4$], and protease inhibitors [Roche]). Anti-PDGFRb (Santa Cruz, 958) was used to immunoprecipitate PDGFRb from whole cell lysate samples containing 0.5 mg protein. Washed immunoprecipitates were subjected to SDS-Page and immunoblotted with anti-PTyr-100 antibody (Cell Signaling, 9411).

### Chromatin Immunoprecipitation

Chromatin Immunoprecipitation (ChIP) experiments were carried out as previously described (Beckerman et al., 2009). Briefly, $KP_{fl}C$ cells were treated with 1% formaldehyde prior to lysis in RIPA Buffer and sonication to yield 500 bp fragments. Protein A/G Sepharose beads were conjugated to anti-NF-YB antibody (Santa Cruz, 13045) which were subsequently used to immunoprecipitate NF-YB from 1 mg whole cell lysate. Quantitative ChIP was carried out on an ABI StepOne Plus using SYBR green dye. Genomic Location of the NF-YB site within the promoter of *PDGFRB* was located using a literature search (Hackzell et al., 2002).

### Immunohistochemistry and Immunofluorescence

Tissues were fixed overnight in formalin, embedded in paraffin, and cut into 5-μm thick sections. Sections were subjected to hematoxylin and eosin staining, and immunohistochemical and immunofluorescent staining following standard protocols. The following primary antibodies were used: mouse anti-GFP (Cell Signaling), rabbit anti-p-PDGFR-β (Tyr 1021) (Santa Cruz Biotechnology), mouse anti-p53 (OP43, Calbiochem) and rat anti-CK8 (DSHB). For immunofluorescence Alexa Fluor 488 goat anti-rabbit and Alexa Fluor 568 goat anti-rat were used as secondary antibodies, and DAPI was used as a chromogen. Images were acquired using a Zeiss Axio Imager D1 scope.

### Mouse Studies

All animal experiments were performed in accordance with a protocol approved by the Memorial Sloan-Kettering Institutional Animal Care and Use Committee. For colonization studies, KPC cells ($1x10^5$) were resuspended in 200 μl PBS and injected intravenously into the tail vein of 8 week-old female athymic nude mice. Lungs were harvested 7 days post injection and analyzed for colonization by GFP positivity (Nikon SMZ1500) and histology.

*Pdx1-Cre* (Hingorani et al., 2003), *LSL-Kras*$^{G12D}$ (Jackson et al., 2001) and *LSL-p53*$^{R172H}$ (Olive et al., 2004) mouse strains were previously described: Male *Pdx1-Cre*$^{+/+}$, *LSL-p53*$^{R172H/R172H}$ mice were bred with female *LSL-Kras*$^{G12D/+}$ mice to generate KPC mice. Strains were maintained on mixed background. Mice were genotyped by polymerase chain reaction analysis as described previously (Hingorani et al., 2005). Mice were dosed twice daily by oral gavage with 50 mg/kg Imatinib in $ddH_2O$ or with $ddH_2O$ only. Organs and tumors were removed and fixed in 10% buffered formalin and tumor and metastatic burden was assessed by gross pathology and histology.

### Human Data Sets

The gene expression data and survival analyses of PDAC patients is from The International Cancer Genome Consortium (ICGC) pancreatic cancer project, which is stored at Gene Expression Omnibus (GEO) with accession number GSE50827. It includes gene expression data from 103 primary tumor samples, 98 of which contain disease-free survival and clinicopathological annotations, and used in the survival analysis according to previously described methods (Biankin et al., 2012).

Gene expression data of ovarian, colorectal, and pancreatic cancer patients with annotated clinical outcomes were downloaded from GEO (GSE9899 [Tothill et al., 2008], GSE17537 [Smith et al., 2010], and GSE28735 [Zhang et al., 2012]). Preprocessed data were downloaded as provided in the data matrix files (GCRMA/RMA normalized Affymetrix expression microarray data) and gene set enrichment analysis (GSEA) was performed on each set after mean-centering across samples. Median of probes per gene was used to account for differential representation on the chip. GSEA analysis was used to evaluate 40-gene signature. For survival analyses, gene expression data was clustered into groups using kmeans and Kaplan-Meier analyses was performed. Significance for these plots was determined using the logrank test.

## SUPPLEMENTAL REFERENCES


Anders, S., and Huber, W. (2010). Differential expression analysis for sequence count data. Genome Biol. *11*, R106.

Biankin, A.V., Waddell, N., Kassahn, K.S., Gingras, M.C., Muthuswamy, L.B., Johns, A.L., Miller, D.K., Wilson, P.J., Patch, A.M., Wu, J., et al.; Australian Pancreatic Cancer Genome Initiative (2012). Pancreatic cancer genomes reveal aberrations in axon guidance pathway genes. Nature *491*, 399–405.

Djebali, S., Davis, C.A., Merkel, A., Dobin, A., Lassmann, T., Mortazavi, A., Tanzer, A., Lagarde, J., Lin, W., Schlesinger, F., et al. (2012). Landscape of transcription in human cells. Nature *489*, 101–108.

Dobin, A., Davis, C.A., Schlesinger, F., Drenkow, J., Zaleski, C., Jha, S., Batut, P., Chaisson, M., and Gingeras, T.R. (2013). STAR: ultrafast universal RNA-seq aligner. Bioinformatics *29*, 15–21.

Hemann, M.T., Fridman, J.S., Zilfou, J.T., Hernando, E., Paddison, P.J., Cordon-Cardo, C., Hannon, G.J., and Lowe, S.W. (2003). An epi-allelic series of p53 hypomorphs created by stable RNAi produces distinct tumor phenotypes in vivo. Nat. Genet. *33*, 396–400.

Jackson, E.L., Willis, N., Mercer, K., Bronson, R.T., Crowley, D., Montoya, R., Jacks, T., and Tuveson, D.A. (2001). Analysis of lung tumor initiation and progression using conditional expression of oncogenic K-ras. Genes Dev. *15*, 3243–3248.

Parkhomchuk, D., Borodina, T., Amstislavskiy, V., Banaru, M., Hallen, L., Krobitsch, S., Lehrach, H., and Soldatov, A. (2009). Transcriptome analysis by strand-specific sequencing of complementary DNA. Nucleic Acids Res. *37*, e123.

Smith, J.J., Deane, N.G., Wu, F., Merchant, N.B., Zhang, B., Jiang, A., Lu, P., Johnson, J.C., Schmidt, C., Bailey, C.E., et al. (2010). Experimentally derived metastasis gene expression profile predicts recurrence and death in patients with colon cancer. Gastroenterology *138*, 958–968.

Tothill, R.W., Tinker, A.V., George, J., Brown, R., Fox, S.B., Lade, S., Johnson, D.S., Trivett, M.K., Etemadmoghadam, D., Locandro, B., et al.; Australian Ovarian Cancer Study Group (2008). Novel molecular subtypes of serous and endometrioid ovarian cancer linked to clinical outcome. Clin. Cancer Res. *14*, 5198–5208.

Zhang, G., Schetter, A., He, P., Funamizu, N., Gaedcke, J., Ghadimi, B.M., Ried, T., Hassan, R., Yfantis, H.G., Lee, D.H., et al. (2012). DPEP1 inhibits tumor cell invasiveness, enhances chemosensitivity and predicts clinical outcome in pancreatic ductal adenocarcinoma. PLoS ONE *7*, e31507.

Zuber, J., McJunkin, K., Fellmann, C., Dow, L.E., Taylor, M.J., Hannon, G.J., and Lowe, S.W. (2011). Toolkit for evaluating genes required for proliferation and survival using tetracycline-regulated RNAi. Nat. Biotechnol. *29*, 79–83.

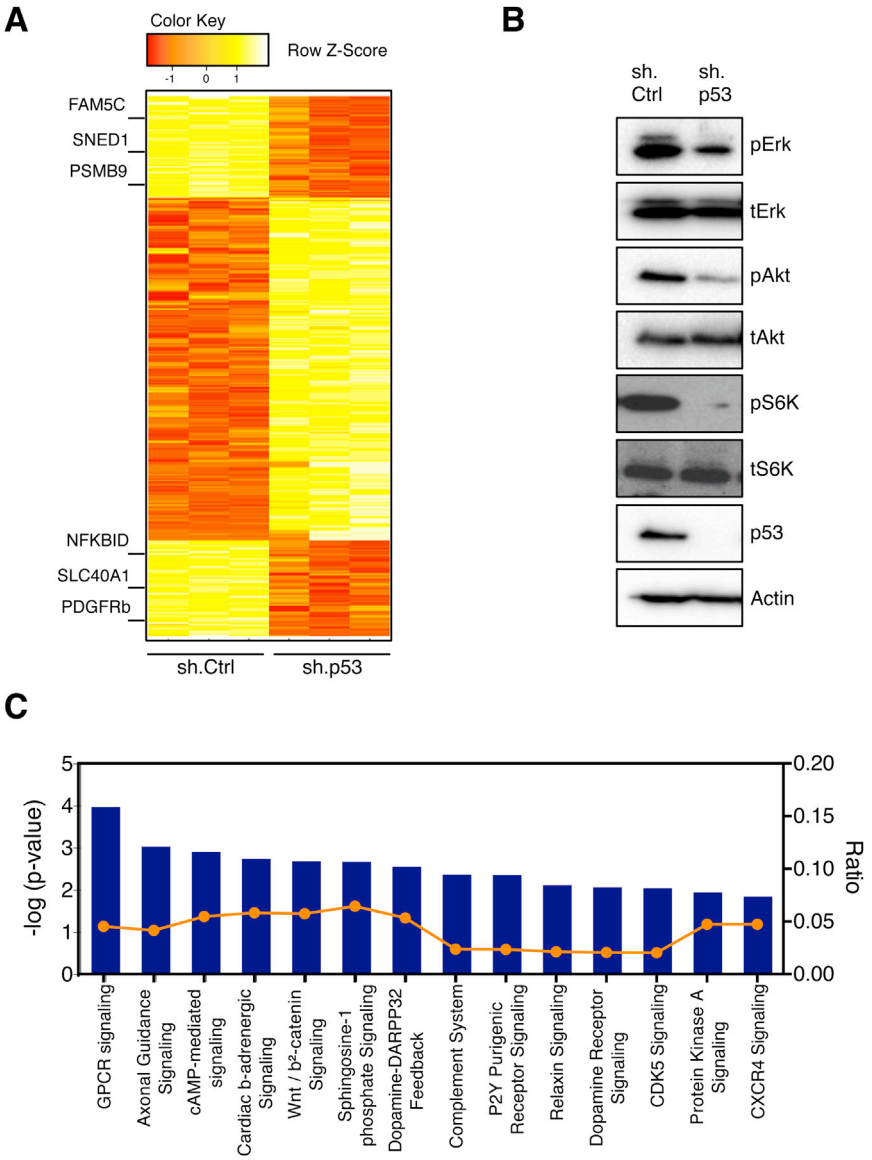


**Figure S1. Knockdown of Mutant p53 in Pancreatic Cancer Cells Alters a Myriad of Genes and Pathways, Related to Figure 2**

(A) Heatmap of significantly changed genes ($p_{adj} < 0.05$) following mutant p53 depletion, as identified by RNA sequencing. Three individual clonal cell lines of KPC+sh.p53 and +sh.Ctrl were analyzed and representative top scoring genes are labeled.

(B) Western blotting analysis of activated downstream PDGF receptor b pathways following knockdown of mutant p53 in KPC cells. Actin expression was used as loading control.

(C) Blue bars that cross the threshold line ($p < 0.05$) represent top scoring pathways that are significantly changed in mutant p53-depleted KPC cells. Data was analyzed through the use of ingenuity pathway analysis.

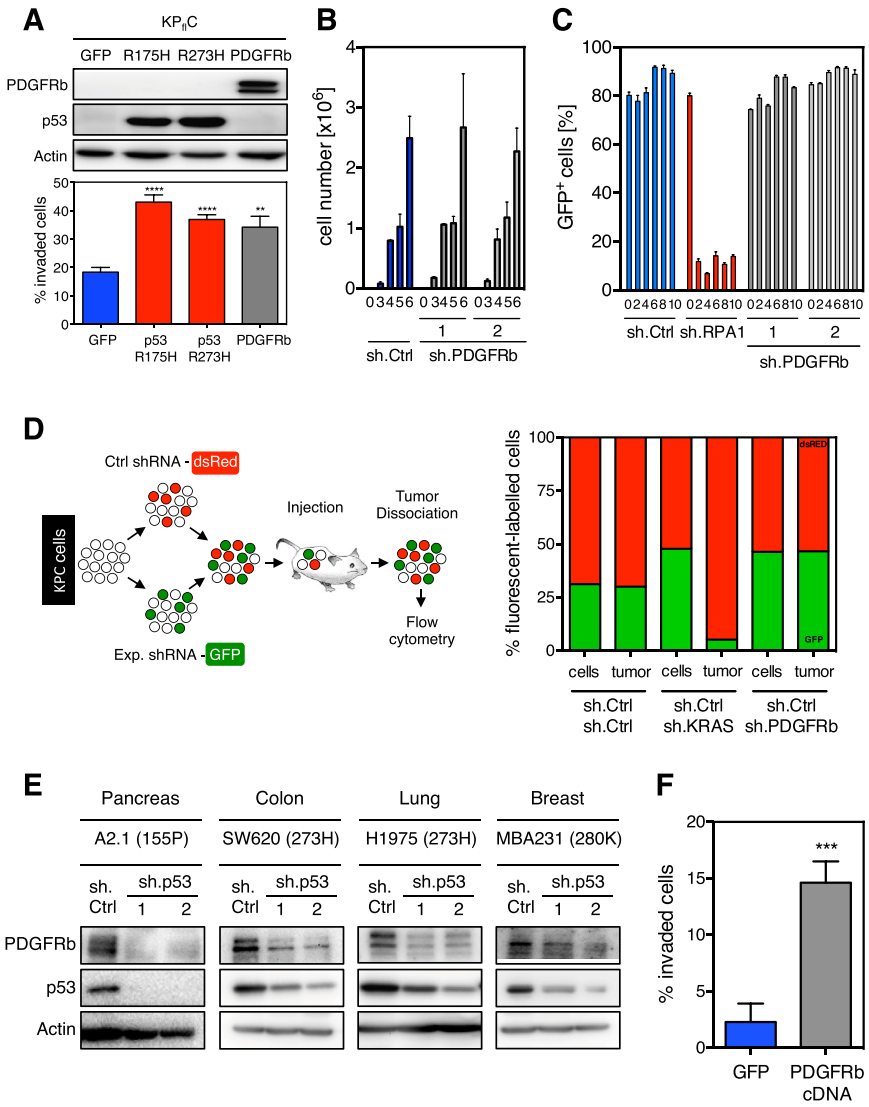


**Figure S2. PDGFRb Expression Levels Depend on p53 Status and Determine the Invasive Ability of Murine and Human Cancer Cells without Affecting Cell Proliferation, Related to Figure 3**

(A) Western blotting analysis of PDGFRb, p53, and actin from $KP_{fl}C$ cells stably expressing a GFP-, $p53^{R175H}$-, $p53^{R273H}$-, or PDGFRb-cDNA vector (upper panel). Quantification of invasion into collagen from the same cells (lower panel). The average of invaded cells from 9 replicates ± SD is shown. **p < 0.01, ****p < 0.0001.

(B) Cell number over time (days) of KPC cells stably expressing sh.Ctrl or sh.PDGFRb (1 or 2). Data presented as mean ± SD.

(C) Negative selection RNAi studies in KPC cells stably expressing dox-inducible sh.Ctrl, sh.RPA3 or sh.PDGFRb (1 or 2) using the tet-on TRMPV system. Graphs represent the percentage of shRNA-expressing ($Venus^+$ $dsRed^+$) cells over time (days), normalized to initial measurement 1 d after dox treatment. Data presented as mean ± SD.

(D) Schematic of dual-color competitive proliferation assay in vivo for evaluating effects of RNAi-mediated PDGFRb suppression in tumor growth. KPC cells were transduced with indicated experimental shRNAs ($GFP^+$) and a neutral control shRNA ($dsRED^+$) (left panel). Percentage of cells expressing indicated experimental shRNA ($GFP^+$) or the neutral control shRNA ($dsRED^+$) in pre-injected cells and tumors 2 weeks after injection. Values represent the mean of multiple pre-injected or tumor-derived cell lines (right panel).

(E) Western blotting analysis of PDGFRb, p53, and actin levels in human pancreatic, colon, lung, and breast cancer cells stably expressing sh.Ctrl or sh.p53 (1 or 2). Mutation of p53 as indicated.

(F) Quantification of the invasion into collagen of human $p53^{-/-}$ ASPC pancreatic cancer cells stably expressing a GFP- or PDGFRb-cDNA vector. The average of invaded cells from 9 replicates ± SD is shown. ***p < 0.001.

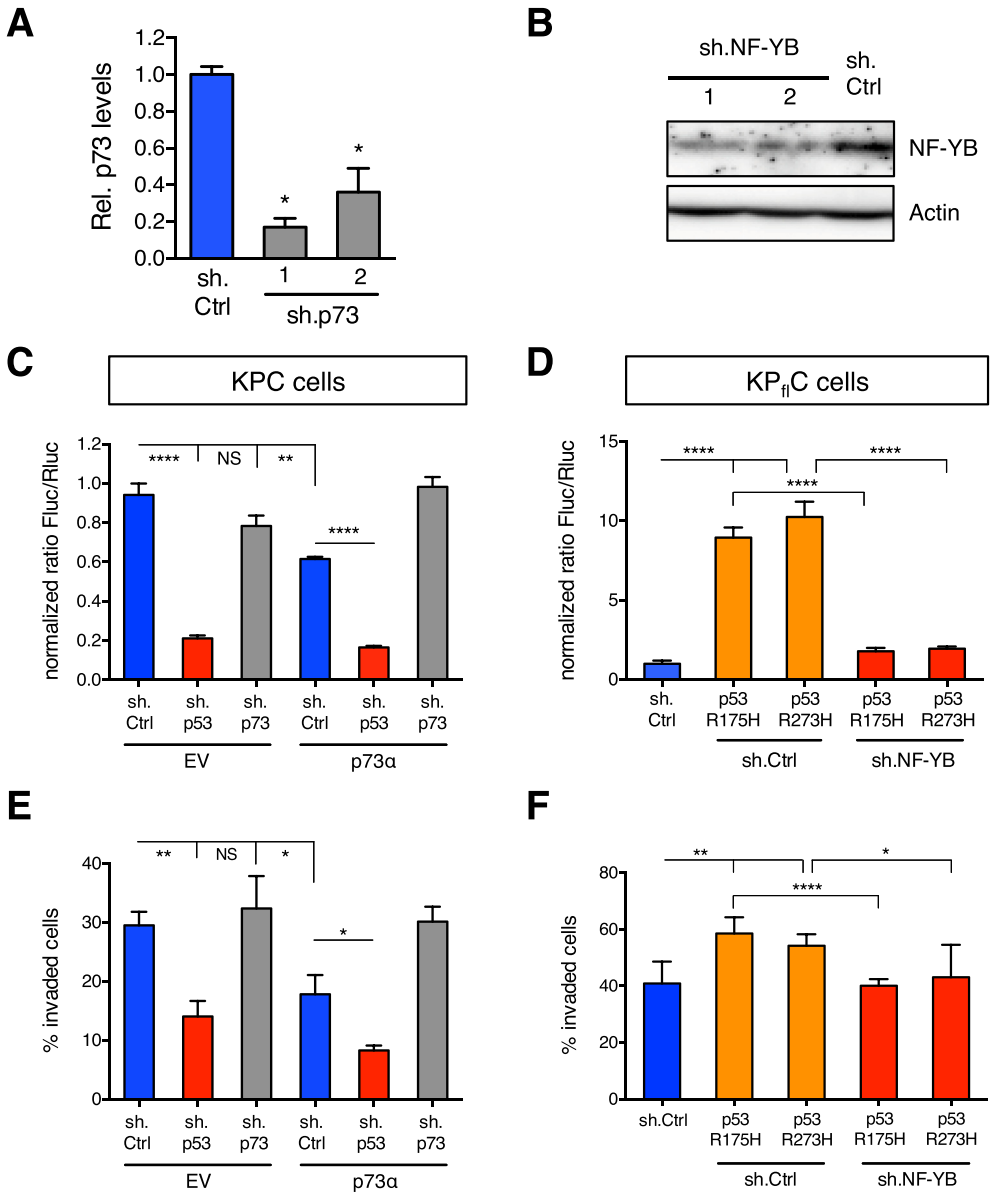


**Figure S3. Mutant p53 Drives *PDGFRB* Transcription by Opposing the Repressive Function of the p73/NF-Y Complex, Related to Figure 4**

(A) qRT-PCR for p73 in KPC+sh.p73 (1 or 2) or +sh.Ctrl cells. Data present mean normalized p73 expression ± SD of triplicate samples. A representative result of three repeated experiments is shown. *p < 0.05.

(B) NF-YB and actin levels of $KP_{fl}C$ cells infected with sh.NF-YB or sh.Ctrl as determined by western blotting.

(C) After double infection using an empty control or HAp73α vector together with sh.Ctrl, sh.p53, or sh.p73, KPC cells were cotransfected with the *PDGFRB*-promoter-luciferase construct and renilla-luciferase vector. Firefly-luciferase activity of GFP-vector cells was set to 1. Values are relative Firefly-luciferase (Fluc) units normalized by renilla expression (Rluc) ± SD of quadruplicate samples. **p < 0.01, ****p < 0.0001. A representative result of three repeated experiments is shown.

(D) $KP_{fl}C$ cells stably expressing sh.Ctrl or sh.NF-YB together with mutant p53 (175H or 273H) were cotransfected with the *PDGFRB*-promoter-luciferase construct and renilla-luciferase vector. Luciferase activity was measured as described above. ****p < 0.0001.

(E) Quantification of invasion of the same cells as in (C). The average of invaded cells from 9 replicates ± SD is shown. A representative result of three repeated experiments is shown. *p < 0.05, **p < 0.01.

(F) Quantification of invasion of the same cells as in (D). The average of invaded cells from 9 replicates ± SD is shown. A representative result of three repeated experiments is shown. *p < 0.05, **p < 0.01, ****p < 0.0001.

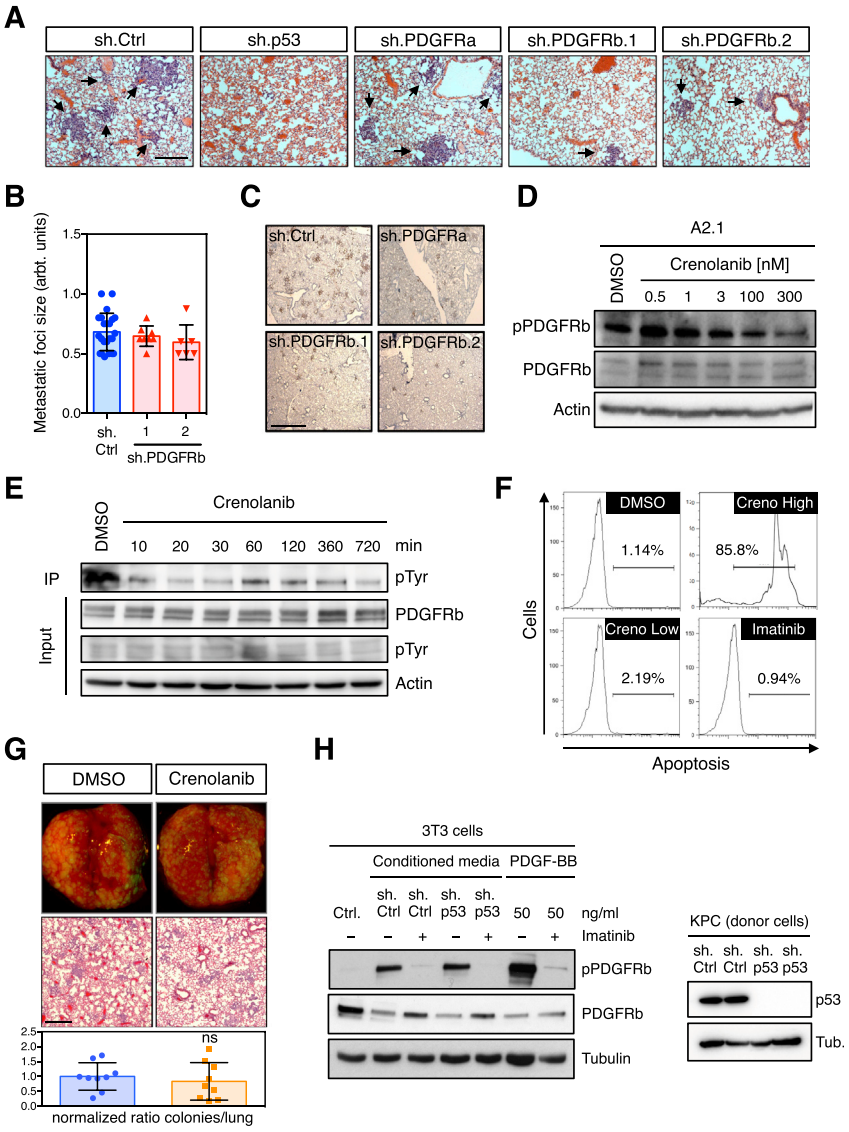


**Figure S4. Inhibition of PDGFRb Activity by RNAi or Small Molecules Decreases Metastatic Potential of Pancreatic Cancer Cells, Related to Figure 5**

(A) Lung colonization assays after tail vein injection of PDGFRa-, PDGFRb (1 or 2)-, p53-, and control-depleted KPC cells. Hematoxylin and eosin (H&E) stains of representative sections of pulmonary lobes from indicated mice are shown, arrows indicate metastases. Scale bars represent 50 μm.

(B) Relative nodule size of lung metastases from mice intravenously injected with PDGFRb (1 or 2)-, and control-depleted KPC cells. Data represent mean ± SD.

(C) GPF immunohistochemistry on histological lung sections from lung colonization assay in (B). shRNA expression correlates with GFP signal, as the fluorescent marker is linked to the hairpin. Scale bars represent 1000 μm.

(D) Western blotting for pPDGFRb, PDGFRb, and actin in human A2.1 cells after treatment with DMSO or crenolanib at varying doses.

(E) Immunoprecipitation of PDGFRb from KPC cells treated with DMSO or crenolanib (300 nM) for different time periods. The input protein levels for PDGFRb, phospho-Tyrosine, and actin and those present in immunoprecipitates for phospho-Tyrosine were determined by western blotting.

(F) Propidium Iodide staining of KPC cells treated overnight with either DMSO, Crenolanib (0.3 (Creno Low) or 25 μM (Creno High)) or imatinib (3 μM).

(G) Lung colonization assays after tail vein injection of crenolanib- or DMSO-treated $KP_{fl}C$ cells. Representative merged brightfield/GFP images of whole lung as well as H&E stains of representative sections of pulmonary lobes are shown. Quantification of total number of lung metastatic nodules in individual mice ($n > 6$) (lower panel). Data presented as mean ± SD. Scale bars represent 100 μm.

(H) Western blotting for pPDGFRb, PDGFRb, and tubulin of starved 3T3 cells, which were pretreated with either DMSO or Imatinib (3 μM) for 4 hr and subsequently stimulated for 15 min with conditioned media from KPC (sh.Ctrl or sh.p53) or 50 ng/μl PDGF-BB (left panel). Western blotting for p53 and tubulin of KPC+sh.Ctrl and +sh.p53 (right panel).

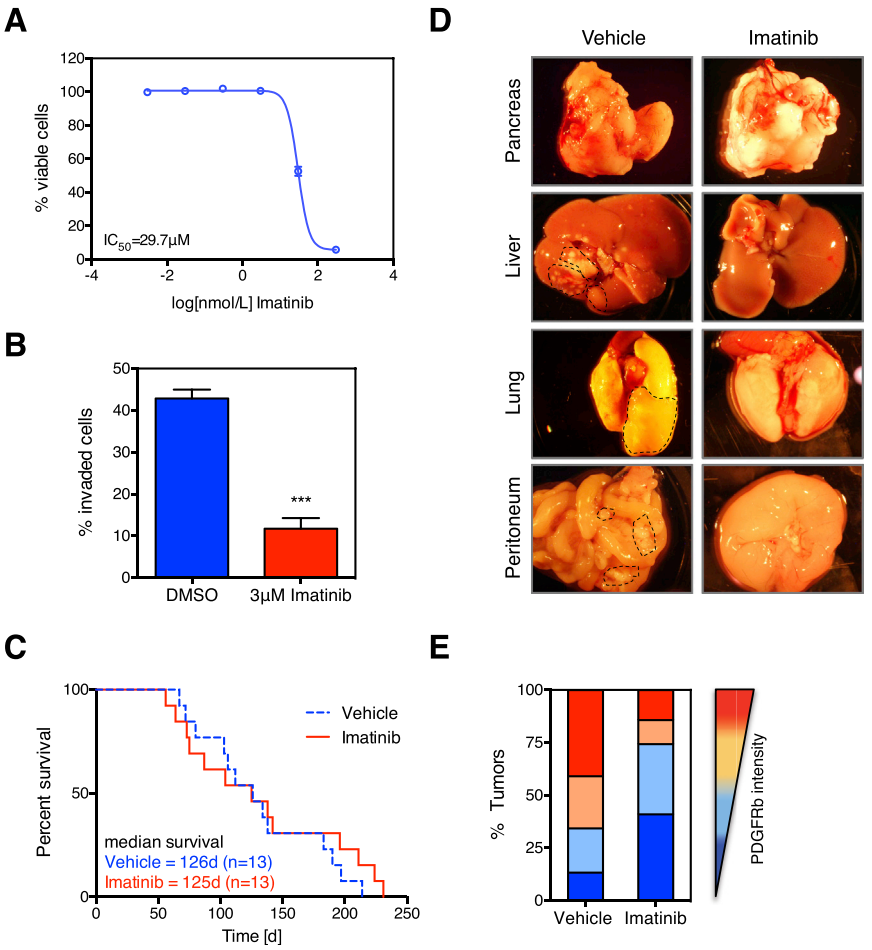


**Figure S5. Imatinib Reduces Invasiveness of KPC Cells and Metastases Formation in KPC Mice, Related to Figure 6**

(A) MTS assay ($E_{490}$) of KPC cells treated with imatinib with various doses for 72 hr. Normalized values are expressed as means ± SD form quadruple replicates.

(B) Quantification of invasion of KPC cells treated with either DMSO or imatinib at 3 μM. The average of invaded cells from 9 replicates ± SD is shown. A representative result of three repeated experiments is shown. ***$p < 0.001$.

(C) Kaplan–Meier survival curves of mice treated with vehicle or imatinib (50 mg/kg) from 8 weeks of age.

(D) Representative bright field images of pancreatic tumor, liver, lung and peritoneum from KPC mice treated with vehicle or imatinib. Black arrows denote metastases.

(E) Quantification of pPDGFRb intensity in pancreatic tumors of KPC mice treated with vehicle or imatinib. pPDGFRb was assessed by immunofluorescence and its intensity scored from 0 (pPDGFRb low levels) to 3 (pPDGFRb high levels). 15 images per tumor from 7 mice per group were analyzed.

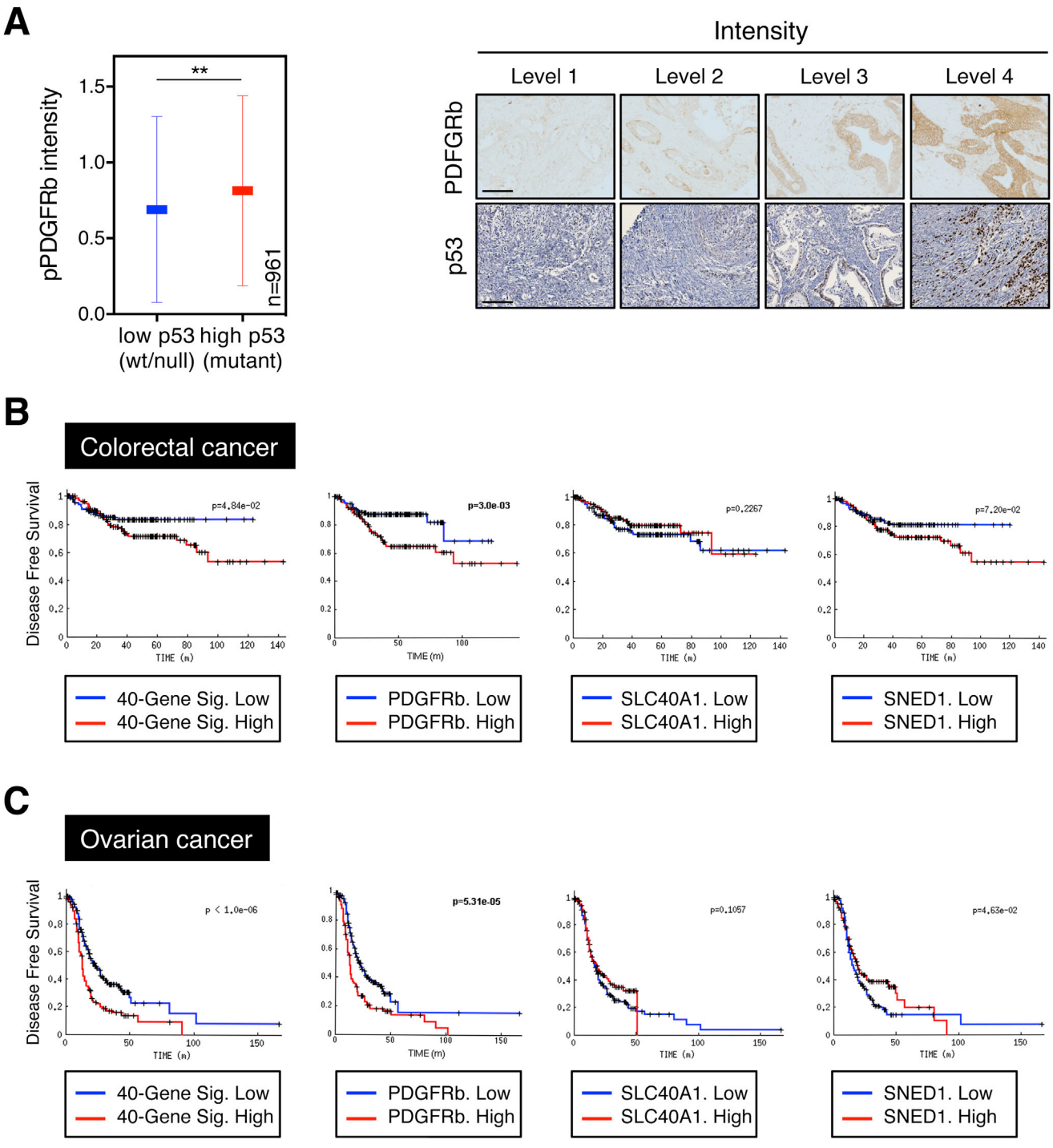


**Figure S6. Metastasis-free Survival of Colorectal and Ovarian Cancer Patients Is Dictated by Mutant p53-Regulated Genes, Related to Figure 7**

(A) pPDGFRb levels in human PDAC samples (n = 961) stratified by p53 (left panel). Levels of pPDGFRb and p53 were determined by IHC and representative images are shown (right panel). **$p < 0.01$. Scale bars represent 100 μm.

(B) Kaplan-Meier survival curves of colorectal cancer patients (clinical variable = DFS) as a function of the expression levels of the 40 genes from the mutant *p53* gene signature, PDGFRb, SLC40A1, and SNED1.

(C) Kaplan-Meier survival curves of ovarian cancer patients (clinical variable = DFS). Patients were stratified as in (B).